

# Dimensional Reduction: A Practical Formalism for Manipulating Solid Structures

Eric G. Tulsy and Jeffrey R. Long\*

Department of Chemistry, University of California, Berkeley, California 94720-1460

Received September 29, 2000. Revised Manuscript Received January 22, 2001

Conceptually, it is not difficult to imagine reaching into a solid structure and carving out just that portion of the framework we desire. Solid-state reactions incorporating an ionic component into a covalent structure have long been recognized as experimental means for accomplishing just such feats. However, the method does not always succeed, and so, in an effort to extend its use in more logical approaches to solid synthesis, we herein provide an assessment of the scope and limitations of the reaction type. Dimensional reduction is set forth as a general formalism describing how the metal–anion (M–X) framework of a parent compound,  $\text{MX}_n$ , is dismantled upon reaction with an ionic reagent  $\text{A}_n\text{X}$  to form a child compound  $\text{A}_n\text{MX}_{x+n}$ . The added anions serve to terminate M–X–M bridges, yielding a less tightly connected framework that retains the metal coordination geometry and polyhedron connectivity mode of the original parent structure. In most instances, the connectedness of the ensuing framework can also be predicted, facilitating enumeration of likely structures. A database containing more than 3000 relevant crystal structures has been compiled (available at <http://alchemy.cchem.berkeley.edu/dimred>) and is employed in evaluating the applicability of dimensional reduction to various systems. Examples are provided and results are tabulated for the deconstruction of parent solids featuring octahedral, tetrahedral, square planar, and linear metal coordination polyhedra linked through corner-, edge-, and face-sharing interactions. The success of dimensional reduction is observed to depend significantly on the choice of the counteranion A (with smaller cations typically giving more reliable results), suggesting that this should be considered a variable parameter when targeting a specific child framework. The utility of the method in dismantling cluster-containing frameworks is also discussed.

## 1. Introduction

Organic chemists have at their disposal a vast library of reaction schemes for performing specific structural transformations. The careful evaluation of the scope and limitations of each reaction—particularly with regard to experimental conditions and functional group compatibility—has enabled development of a logic by which complex organic structures can be built up from simpler components.<sup>1</sup> In stark contrast, solid-state chemists have in their grasp only a few generalizable reaction schemes with which to modify the structure of an inorganic solid in a manner that might be predicted a priori. Consequently, a similar logic for constructing solids has failed to emerge, despite the obvious advantages of wielding such an approach to tune physical properties that correlate so critically with the structure of a solid material. In an effort to help alleviate this discrepancy and extend the library of solid-state reactions, we herein formalize and evaluate a long-standing means of manipulating binary solid frameworks.

Owing to the extreme variation of bonding interactions in inorganic structures, solid-state synthesis has

traditionally been a discipline rife with preparative techniques, but lacking in predictive capability.<sup>2</sup> For even very simple solids, fundamental issues such as understanding mechanisms of formation<sup>3</sup> and determining stable compositions<sup>4</sup> and crystal structures<sup>5</sup> remain as challenges for ongoing research. While the prospect of gaining kinetic control in the synthesis of solids through the use of low-temperature sol–gel,<sup>6</sup> molten salt,<sup>7</sup> or solventothermal<sup>8</sup> techniques has excited considerable interest,<sup>2bc</sup> these methods typically do not prescribe the overall structure of the resultant metastable product. What predictive reaction schemes do exist are easily enumerated. Intercalation reactions involve the insertion of guest species into existing interstices within a solid host.<sup>9</sup> Related ion exchange reactions entail the interchange of ions, again without disrupting the covalent framework of the solid host.<sup>10</sup> Other soft chemical (or *chimie douce*) routes, classified as topotactic condensation reactions, alter the framework itself by forging new bonds between surfaces upon elimination of intervening terminal ligands.<sup>11,12</sup> Often, the very existence of a framework will suggest the possibility of synthesizing isostructural variants by



radii remain approximately constant, such that the directional bonding between M and X in the parent and child compounds is expected to be similar. As we shall see, in some cases the availability of additional anions X or association of the framework with external counterions A will enforce a structure not in accord with the foregoing predictions, but often these effects can be minimized through the judicious selection of an alternative A cation (see section 5 below). Indeed, because the more covalent M–X framework is generally of primary interest, the choice of A in reaction (1) should be viewed as an experimental variable, equivalent in some regards to adjusting the physical conditions under which an organic reaction is performed.

Importantly, one can further predict the *connectedness* of the child compound framework, which we define here as the mean number of distinct M–X–M linkages around the metal centers.<sup>18</sup> In other words, it is the average number of bonds that must be severed to liberate a discrete  $\text{MX}_{\text{CN}_M}$  polyhedron, where  $\text{CN}_M$  is the metal coordination number. If  $\text{CN}_X$  denotes the number of M atoms coordinated to X, then  $(\text{CN}_X - 1)$  M–X–M linkages extend from a given metal center through the coordinated anion. The connectedness is calculated by summing the number of linkages extending from a center  $M_i$  through all  $\text{CN}_{M_i}$  of its coordinated anions  $X_j$  and then averaging the sums obtained for each of the  $m$  different metal centers in a repeat unit:

$$\text{connectedness} = \frac{1}{m} \sum_{i=1}^m \sum_{j=1}^{\text{CN}_{M_i}} (\text{CN}_{X_j} - 1) \quad (2)$$

For frameworks containing only one type of metal and one type of anion, this expression simplifies to  $\text{CN}_M \times (\text{CN}_X - 1)$ . In such cases, the ratio of anions to metals (which is  $x + n$  for a compound  $\text{A}_{na}\text{MX}_{x+n}$ ) must be equal to  $\text{CN}_M/\text{CN}_X$ .<sup>19</sup> Hence, the connectedness for these simple valence or *haplotype*<sup>20</sup> frameworks can be deduced from just  $\text{CN}_M$  and the chemical formula

$$\text{haplotype connectedness} = \text{CN}_M \times \left( \frac{\text{CN}_M}{x+n} - 1 \right) \quad (3)$$

For example, the rock salt (NaCl) lattice, with six-coordinate metal centers, has a connectedness of  $6 \times (6/1 - 1) = 30$ , while the fluorite ( $\text{CaF}_2$ ) lattice, with eight-coordinate metal centers, has a connectedness of  $8 \times (8/2 - 1) = 24$ .

As is the case for the structures depicted in Figure 1, many child compounds exhibit frameworks composed of  $\text{MX}_{\text{CN}_M}$  polyhedra with each vertex shared between no more than two metal centers (i.e., with anions restricted to coordination numbers of one or two). Under this restriction, frameworks with  $(x + n)$  anions per metal center must have an average of  $2 \times [\text{CN}_M - (x + n)]$  two-coordinate X anions bound to each M atom. And since each two-coordinate anion provides a single M–X–M linkage, the connectedness for such compounds is precisely that average. Thus, the connectedness of the framework in a child compound,  $\text{A}_{na}\text{MX}_{x+n}$ , derived from a parent compound featuring only one- and two-coordinate anions is predicted to be

$$\text{connectedness} = 2 \times [\text{CN}_M - (x + n)] \quad (\text{for } \text{CN}_X \in \{1, 2\}) \quad (4)$$

Using eq 4, the connectedness of the  $\text{MX}_3$  framework **1** is calculated as  $2 \times [6 - (3 + 0)] = 6$ , in agreement with the structure wherein each of the six vertices of the  $\text{MX}_6$  octahedra are involved in just one M–X–M linkage. Increasing  $n$  by 1 decreases the connectedness by 2, so the framework in a child compound with formula  $\text{A}_a\text{MX}_4$  ( $n = 1$ ) is predicted to have a connectedness of 4. Framework **2** achieves this result by surrounding each metal center with four M–X–M bridges and two terminal X ions. Also consistent, framework **3** of  $\text{A}_{2a}\text{MX}_5$  ( $n = 2$ ) has two bridges per metal center, for a connectedness of 2, and the saturated framework **4** of  $\text{A}_{3a}\text{MX}_6$  ( $n = 3$ ) is zero-connected.

Based on knowledge of the parent structure, the connectedness expected for most child compounds can be calculated through a process analogous to that just described. However, for compounds with anions liable to assume more than two different coordination numbers, the connectedness cannot be definitively predicted without further specific structural information. As an instructive example, consider the compounds  $\text{NaMnCl}_3$  and  $\text{NH}_4\text{CdCl}_3$ , featuring frameworks **5** and **6**, respectively (see Figure 2).<sup>21,22</sup> The corresponding parent compounds,  $\text{MnCl}_2$  and  $\text{CdCl}_2$ , both adopt twelve-connected haplotype structures with two-dimensional sheets of octahedra each sharing six edges.<sup>23,24</sup> An  $\text{AMCl}_3$  child compound should then have less tightly connected frameworks of edge-sharing octahedra, but because the chloride anions might reasonably adopt coordination numbers of one, two, or three, its connectedness is not uniquely determined. Since the anion:metal ratio must equal the ratio of the mean coordination numbers of M and X,<sup>19</sup> it follows that the mean coordination number of Cl in these structures must be  $6/3 = 2$ . In  $\text{NaMnCl}_3$ , this is accomplished with framework **5** in which all chloride anions are two-coordinate, forming six-connected haplotype sheets of edge-sharing octahedra. In  $\text{NH}_4\text{CdCl}_3$ , however, a more complicated edge-sharing structure is realized with framework **6**, consisting of one-dimensional chains in which each metal center is bound by one terminal anion, two anions that are two-coordinate, and three anions that are three-coordinate. The mean anion coordination number is still two, but each metal center is now surrounded by  $(1 \times 0) + (2 \times 1) + (3 \times 2) = 8$  M–Cl–M bridges, for a connectedness of eight. Thus, while the framework connectedness is always seen to be lowered in a child compound, for situations such as this it cannot be quantitatively predicted. Regardless of the precise connectedness, increasing the anion:metal ratio without changing the metal coordination number *must* decrease the mean anion coordination number, resulting in the termination of intermetal M–X–M bridges (see example in Figure 3).<sup>25</sup>

Dimensional reduction can be used to formulate reactions targeting new compounds of altered connectedness (and dimensionality). Scheme 1 shows an array of compounds that might be accessible via dimensional reduction of suitable parent solids containing six-coordinate metal centers. Although the generic formulas listed correspond to common framework compositions,

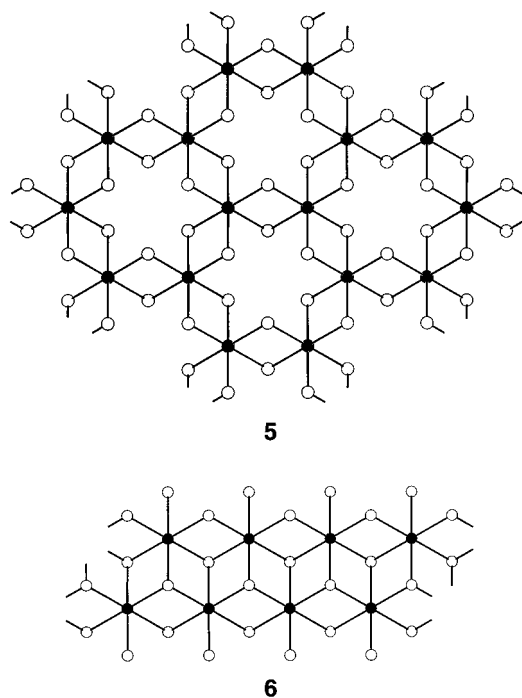


**Figure 2.** Framework isomerism. The two frameworks depicted have identical metal coordination geometry, mode of connectivity, and metal:anion ratio, yet **5** forms six-connected sheets, while **6** forms eight-connected one-dimensional double chains.

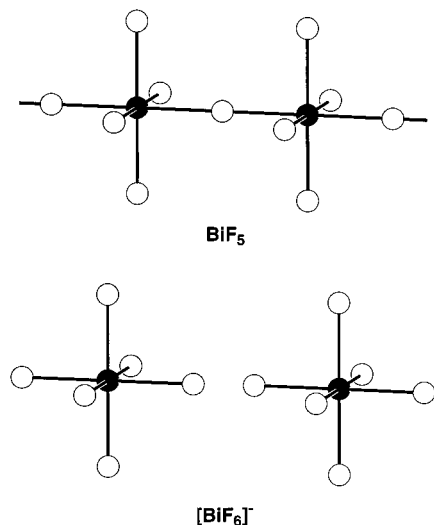
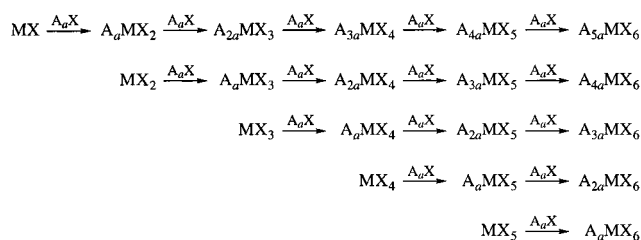


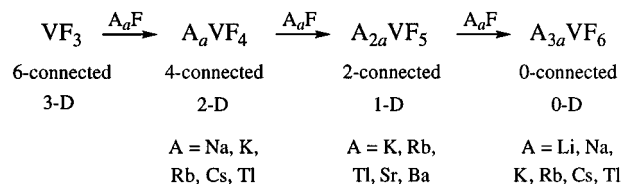
**Figure 3.** Chains of corner-sharing octahedra in BiF<sub>5</sub> (top) incorporate additional fluoride ions upon reaction with AF (A = alkali metal). To maintain the metal coordination geometry while increasing the number of anions, the anion coordination number must be lowered, resulting in the termination of Bi–F–Bi bridging interactions. One can envision this as occurring through a process in which each added fluoride ion inserts into a Bi–F bond. However, it is important to emphasize that dimensional reduction is not intended as a specific reaction mechanism, but only as an empirical link between the structures of related compounds.

the products do not necessarily have to occur at discrete steps of  $n = 1$  as shown. Rather, related child compounds are possible for any rational value of  $n$  between 0 and  $6 - x$ . To illustrate this and one other point, we shall examine the dimensional reduction of VF<sub>3</sub>, which adopts the structure of framework **1** (see Figure 1), with

### Scheme 1



### Scheme 2<sup>a</sup>



<sup>a</sup> For compounds with alkali metals or Tl cations,  $a = 1$ , while for those with alkaline earth metal cations,  $a = 0.5$ .

VF<sub>6</sub> octahedra sharing corners in all three dimensions.<sup>26</sup> Dimensional reduction predicts that reaction with A<sub>a</sub>F should yield child compounds with corner-sharing octahedra in frameworks of lower connectedness, as evaluated using eq 4 above ( $\text{CN}_M = 6$ ,  $x = 3$ ). Thus, by performing a solid-state reaction between VF<sub>3</sub> and A<sub>a</sub>F in a 1:1 molar ratio, one can target a compound A<sub>a</sub>VF<sub>4</sub> with VF<sub>6</sub> octahedra sharing corners to form a four-connected framework (such as **2**). Analogous reactions employing a 1:2 and 1:3 molar ratio would target A<sub>2a</sub>VF<sub>5</sub> with a two-connected framework (such as **3**) and A<sub>3a</sub>VF<sub>6</sub> with discrete zero-connected octahedral anions (**4**), respectively. Indeed, many of these compounds have been prepared by just this route (see Scheme 2), including the entire series with A = K, Rb, Tl.<sup>27</sup> However, one can also imagine using dimensional reduction to produce structures intermediate to those depicted in Figure 1. For instance, one-dimensional multichains consisting of  $m$  parallel chains of type **3** fused via corner sharing could be targeted in  $(4 - 2/m)$ -connected  $A_{(m+1)a}V_mF_{4m+1}$  child compounds by employing an  $m:(m+1)$  ratio of reactants. Even more complicated intermediate structures are observed in the vanadium(III)–fluoride system (see Figure 4). The two-dimensional solid K<sub>5</sub>V<sub>3</sub>F<sub>14</sub> (**7**),<sup>28</sup> features four-connected corner-sharing octahedra linked through two-connected octahedra to form a square net. Since the structure contains two two-connected octahedra per four-connected octahedron, its overall connectedness, which is the *mean* degree of connectivity, is  $(2 + 2 + 4)/3 = 8/3$ . Similarly, Rb<sub>2</sub>V<sub>5</sub>F<sub>17</sub> displays a mixture of five- and six-connected octahedra that share corners in a two-dimensional framework (**8**) with a connectedness of  $26/5$ .<sup>27</sup>

Although dimensional reduction predicts the coordination geometry of M, the polyhedron connectivity mode, and the connectedness of a framework, for most cases multiple isomers are possible within these constraints. The likely isomeric structures are expected to be similar locally for both M and X, so differences between them will depend largely on the choice of counteranion A and on packing considerations. Indeed, the frameworks depicted in Figure 1 are by no means

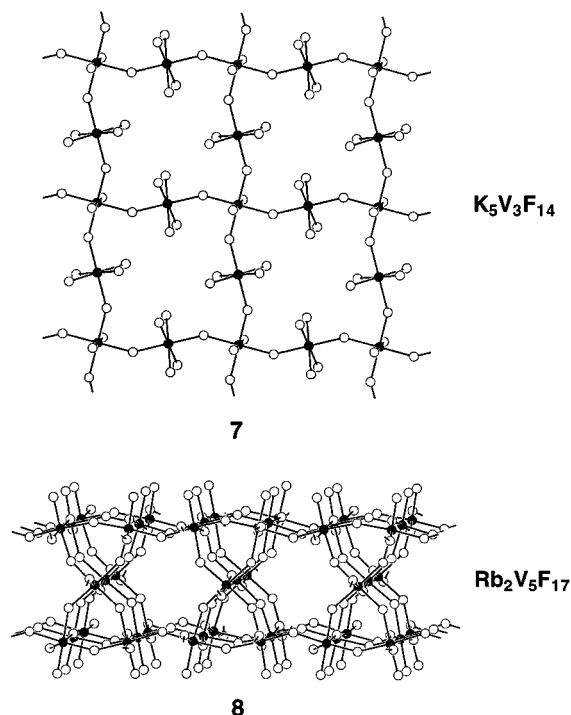


**Figure 4.** Vanadium fluoride frameworks with nonintegral connectedness. In **7**, a mixture of two- and four-connected corner-sharing octahedra form sheets of connectedness  $(2 + 2 + 4)/3 = 8/3$ . In **8**, corner-sharing octahedra form a two-dimensional structure with a layer of six-connected octahedra sandwiched between two layers of five-connected octahedra. With four five-connected octahedra per six-connected octahedron, the connectedness is  $(4 \times 5 + 1 \times 6)/5 = 26/5$ .

unique for the compositions given. Consider the potential structures for  $A_{2a}VF_5$ , which, as a child compound derived from  $VF_3$  (**1**), is expected to exhibit a two-connected framework composed of corner-sharing  $VF_6$  octahedra. The expectations are most simply satisfied by a linear chain of octahedra sharing trans corners (**3**), as observed in the structures of  $A_2VF_5$  ( $A = Rb, Tl$ ).<sup>27</sup> However, other more complicated frameworks also meet the criteria and are frequently observed upon varying the A constituent. Some examples are shown in Figure 5. The octahedra in the analogous  $K_2VF_5$  compound share cis corners instead of trans, resulting in an isomeric zigzag chain (**9**).<sup>27</sup> Similar local interactions are present within the framework of  $Pb_3V_2F_{12}$  ( $=PbVF_5 \cdot \frac{1}{2}PbF_2$ ), where  $VF_6$  octahedra are again linked through cis corners, in this case forming discrete square  $[V_4F_{20}]^{8-}$  ions (**10**) that cocrystallize with excess  $PbF_2$ .<sup>27</sup> The structure of  $BaVF_5$  is unusual in that it features two different isomeric chains.<sup>27</sup> One of the chains adopts the two-connected linear structure of **3**, while the other exhibits two one-connected octahedra per four-connected octahedron (**11**), for a mean degree of connectivity of  $(1 + 1 + 4)/3 = 2$  in the adorned chain and an overall connectedness of two. Note that none of the two-connected frameworks in Figure 5 possess more than two distinct metal sites.

An infinite array of isomers can be generated by making alterations of this sort; however, as we shall see, nature typically selects one of the simpler possible frameworks. Consequently, specifying the composition, metal coordination geometry, polyhedron connectivity

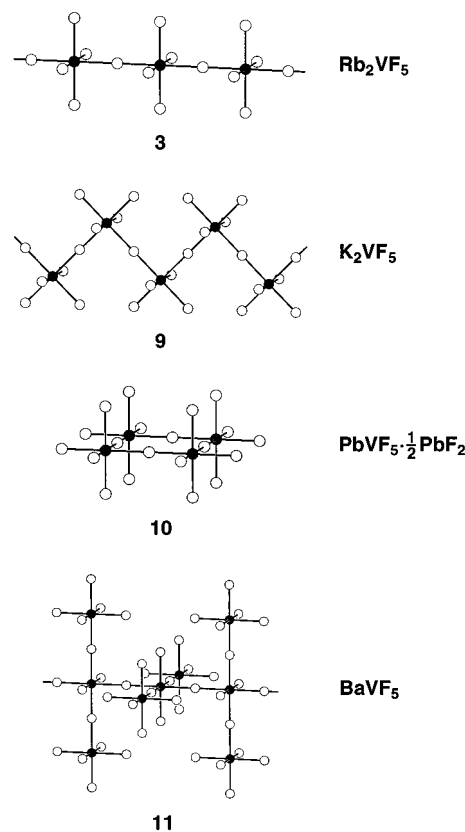


**Figure 5.** Isomeric  $[VF_5]^{2-}$  two-connected frameworks of corner-sharing octahedra. Each framework fits with the predictions of dimensional reduction, yet variation of local connectivity yields these distinct structures. The structures have been idealized for clarity; actual V–F–V angles are close to the  $149^\circ$  angle observed in  $VF_3$ .<sup>26</sup>

mode, and connectedness of a framework severely limits the number of structure types commonly observed. Given the composition, dimensional reduction then dictates the other three specifications, and can therefore be used to identify a small set of known structures that a new compound is most likely to adopt. For example, while many compounds have the composition  $AMX_3$ , most adopt one of only a few common structure types: perovskite ( $CaTiO_3$ ),<sup>29</sup>  $NH_4CdCl_3$ ,<sup>22</sup>  $BaNiO_3$ ,<sup>30</sup> or wollastonite ( $CaSiO_3$ ).<sup>31</sup> The constraints that dimensional reduction places on such a child compound permit ready distinction between these structures for a given choice of A, M, and X. Moreover, our examination of the scope of dimensional reduction has produced a database that can be used to identify *all* of the known structures meeting a specified set of constraints. Hence, dimensional reduction will provide a rapid empirical means of guessing a structure, which could on occasion preclude extensive computation—despite recent advances in the development of theoretical methods for predicting solid structures.<sup>5</sup> Other empirical methods of this sort employ structure field maps for evaluating structures of binary compounds,<sup>32</sup> but only rarely can these be applied to ternary compounds.<sup>33</sup> Ultimately, rather than rely upon existing structures, one may wish to exploit a particular parent structure for generating likely child frameworks using an approach analogous to that developed for enumerating molecular cluster geometries.<sup>34</sup>

H																	He
Li	Be										B	C	N	O	F	Ne	
Na	Mg										Al	Si	P	S	Cl	Ar	
K	Ca	Sc	Ti	V	Cr	Mn	Fe	Co	Ni	Cu	Zn	Ga	Ge	As	Se	Br	Kr
Rb	Sr	Y	Zr	Nb	Mo	Tc	Ru	Rh	Pd	Ag	Cd	In	Sn	Sb	Te	I	Xe
Cs	Ba	La	Hf	Ta	W	Re	Os	Ir	Pt	Au	Hg	Tl	Pb	Bi	Po	At	Rn

**Figure 6.** Choices of A, M, and X. Elements shaded light gray were used as potential counterions A in our survey, while those shaded black were used as metals M and those that are white were used as anions X. Dark gray indicates that an element was not used as any of these. Lanthanide elements (not shown) were also used as A cations when appropriate. Some elements, such as zinc, can serve as either A or M.

### 3. Compilation of Proven Structures

A sizable body of experimental data is required for a thorough evaluation of any empirical reaction scheme. Accordingly, a survey of all available structures that could potentially be related through dimensional reduction was undertaken. To ensure the integrity of the data, the survey was limited to compounds whose structures have been proven rigorously by crystallographic means. The resulting database will be used to enumerate systems where dimensional reduction is most applicable as well as to elucidate the causes of any systematic violations of its predictions.

Data were gathered primarily from the Inorganic Crystal Structure Database,<sup>35</sup> Powder Diffraction File,<sup>36</sup> and Dictionary of Inorganic Compounds,<sup>37</sup> which were exhaustively searched for structurally proven binary compounds  $\text{MX}_x$ . These parent structures were classified according to metal coordination geometry, polyhedron connectivity mode, and connectedness. The data sources were then searched for all ternary compounds with formulas  $\text{A}_{na}\text{MX}_{x+n}$  such that  $\text{MX}_x$  has a known unsaturated framework. Choices for A, M, and X were restricted based on the requirements of dimensional reduction (see Figure 6). Thus, X can be any element capable of bridging between metal centers. Our survey, however, encompassed only compounds where X is a halide, oxide, or chalcogenide ion since the paucity of data in other systems (nitrides, phosphides, etc.) prevents us from drawing statistically valid conclusions. The cation A is presumed to have little covalent interaction with X and can therefore be any highly electropositive element, particularly one with a closed shell electron configuration (e.g., alkali metals,  $\text{Tl}^{\text{I}}$ ,  $\text{Cd}^{\text{II}}$ , etc.). Relative to A, M can then be any metal expected to form significantly more covalent interactions with X. Certain compounds were also excluded from the study as a result of characteristics deemed incompatible with dimensional reduction at this basic level. For example, frameworks with anion–anion (X–X) bonding were excluded as parent compounds due to the added complication of possibly severing anion–anion bonds in the course of a reaction. Other omitted parent compounds include nonstoichiometric phases and mixed-valence compounds. For polymorphic compounds, only the ther-

**Table 1. Number of Compounds in the Dimensional Reduction Database**

metal, M	anion, X				total
	oxide	chalcogenide	fluoride	lower halide	
transition metal	970	331	451	450	2202
main group metal	348	284	95	92	819
total	1318	615	546	542	3021

modynamically stable phase under standard conditions was considered.

In all, 524 binary compounds and 2497 ternary compounds were incorporated into the database. Under the aforementioned restrictions, 312 different combinations of M and X and 10056 combinations of A, M, and X are allowed. Note that most metals M can assume multiple oxidation states and that for any one of these the A–M–X phase diagram will contain perhaps four or more distinct phases. Thus, it is quite evident that while our knowledge of the structures of binary compounds is substantial, the exploration of ternary structures has only just begun. Table 1 summarizes the distribution of known structures, a large fraction of which consist of transition metal oxides and fluorides. The complete database can be accessed via the World Wide Web at <http://alchemy.cchem.berkeley.edu/dimred>.

### 4. Examining the Scope of Dimensional Reduction

The database of binary and ternary structures allows us to assess the general effectiveness of dimensional reduction. The structure of each compound of the type  $\text{A}_{na}\text{MX}_{x+n}$  was examined and compared to that of the corresponding  $\text{MX}_x$  parent compound to ascertain whether it follows the tenets of dimensional reduction. For an unsaturated ternary compound, this requires that both the metal coordination geometry and the mode of connectivity match those in the parent compound, thereby allowing prediction of the connectedness in most cases. In contrast, a saturated child compound needs to maintain only the metal coordination geometry of its parent, as all connections have been severed. These two types of compounds will be treated separately in most instances, and emphasis will be placed on the unsaturated compounds, whose structures are less easily pre-

dicted by other means. Compounds were sorted according to parent compound structure type and examined for trends that would suggest how dimensional reduction can be most successfully employed.

**4.1. Frameworks with Corner-Sharing Octahedra.** The set of binary compounds with structures composed strictly of corner-sharing octahedra contains 41 metal fluorides and 2 metal oxides ( $\text{WO}_3$  and  $\text{ReO}_3$ ), all of which are relatively ionic in character. No binary metal chalcogenides or lower halides are included. Pauling's rules attribute the preference for corner-sharing interactions over edge- or face-sharing interactions in ionic compounds to the increase in Coulombic repulsion that arises from the shortened intermetal distance in an edge- or face-bridged structure.<sup>38</sup> Indeed, 75% of all binary and ternary metal fluorides with unsaturated frameworks display only corner-bridging interactions, while only 8% display no such interactions. The preference for octahedral (or higher) coordination of the metal centers in ionic compounds has been attributed to the nondirectionality of ionic interactions; rather than form a few directional covalent bonds, the metal cations surround themselves with as many anions as possible.<sup>38,39</sup> Consequently, the largest spherically symmetric M ions achieve coordination numbers greater than six (as in  $\text{TlF}_3$ ,  $\text{LaF}_3$ , and  $\text{HfF}_4$ ); however, by far the majority of transition metal fluorides exhibit octahedral coordination of the metal. Since there is a clear predisposition for metal fluorides to form structures with corner-sharing octahedra, dimensional reduction applies remarkably well here: 80% (235/294) of all child compounds derived from parent compounds with corner-sharing octahedra have the predicted structural characteristics.

Parent compounds of formula  $\text{MX}_3$  that adopt structures with corner-sharing octahedra are particularly amenable to dimensional reduction. These structures feature  $\text{MX}_6$  octahedra linked through all six corners to form a six-connected three-dimensional framework, as in the  $\text{RhF}_3$  and  $\text{ReO}_3$  (**1**) structure types.<sup>40</sup> The distinction between the two structure types lies solely in the  $\text{M-X-M}$  bond angle and is disregarded here since such attributes, although sometimes retained, do not affect our immediate predictions for child compounds. The known child frameworks that derive from these  $\text{MX}_3$  parent structures via dimensional reduction are enumerated in Table 2. Here, frameworks that are topologically equivalent are grouped together, while frameworks of distinct connectivity (such as the examples depicted in Figure 5) are listed separately. This leads to compounds such as  $\text{Rb}_2\text{VF}_5$  and  $\text{CaCrF}_5$  being grouped together; even though their crystal structures differ, the  $\text{M-F}$  frameworks in the two compounds are superimposable.<sup>27,53</sup> Table 2 serves as a catalog of frameworks that might be attainable by dimensional reduction of any such parent compound. Many systems follow the sequence shown in Figure 1, with framework **9** frequently substituting for framework **3** (see Scheme 2 for examples). Of course, a specific system is not likely to form compounds with every framework listed and may in fact form compounds with frameworks not yet known; nevertheless, the listing provides a useful guideline for the range of likely structures. Note that, in proceeding down the table, the number of equivalents

**Table 2. Frameworks Derived from  $\text{MX}_3$  Compounds with Corner-Sharing Octahedra**

formula	conn.	dim.	no.	examples	ref
$\text{MX}_3$ ( <b>1</b> )	6	3-D	21	$\text{VF}_3$ , $\text{RhF}_3$ , $\text{ReO}_3$	26, 40
$\text{A}_2\text{M}_4\text{X}_{13}$	5.5	3-D	1	$\text{K}_2\text{W}_4\text{O}_{13}$	41
$\text{AM}_3\text{X}_{10}$	5.33	3-D	1	$\text{NaMn}_3\text{F}_{10}$	42
$\text{A}_2\text{M}_5\text{X}_{17}$ ( <b>8</b> )	5.2	2-D	7	$\text{Rb}_2\text{V}_5\text{F}_{17}$ , $\text{Rb}_2\text{Fe}_5\text{F}_{17}$	27, 43
$\text{AMX}_4$ ( <b>2</b> )	4	2-D	25	$\text{RbVF}_4$ , $\text{NaTiF}_4$	27, 44
$\text{AMX}_4$	4	1-D	3	$\text{CsAlF}_4$ , $\text{KCrF}_4$	45
$\text{AMX}_4$	4	2-D	2	$\text{NaCrF}_4$ , $\text{NaFeF}_4$	46
$\text{AMX}_4$	4	2-D	1	$\text{LiInF}_4$	47
$\text{AMX}_4$	4	2-D	1	$\text{KScF}_4$	48
$\text{A}_3\text{M}_2\text{X}_9$	3	2-D	2	$\text{Ba}_3\text{Re}_2\text{O}_9$	49
$\text{A}_5\text{M}_3\text{X}_{14}$ ( <b>7</b> )	2.67	2-D	5	$\text{K}_5\text{V}_3\text{F}_{14}$ , $\text{Na}_5\text{Al}_3\text{F}_{14}$	28, 50
$\text{A}_5\text{M}_3\text{X}_{14}$	2.67	2-D	1	$\text{Na}_5\text{Mn}_3\text{F}_{14}$	51
$\text{A}_{2a}\text{MX}_5^a$ ( <b>9</b> )	2	1-D	17	$\text{K}_2\text{VF}_5$ , $\text{Ba}_2\text{WO}_5$	27, 52
$\text{A}_{2a}\text{MX}_5^a$ ( <b>3</b> )	2	1-D	15	$\text{Rb}_2\text{VF}_5$ , $\text{CaCrF}_5$	27, 53
$\text{AMX}_5$ ( <b>3</b> + <b>11</b> )	2	1-D	5	$\text{BaVF}_5$ , $\text{BaFeF}_5$	27, 54
$\text{AMX}_5 \cdot \frac{1}{2}\text{AX}_2$ ( <b>10</b> )	2	0-D	3	$\text{Pb}_3\text{V}_2\text{F}_{12}$ , $\text{Pb}_3\text{Fe}_2\text{F}_{12}$	27, 55
$\text{A}_4\text{M}_3\text{X}_{15}$	2	1-D	1	$\text{Nd}_4\text{W}_3\text{O}_{15}$	56
$\text{A}_{3a}\text{MX}_6^a$ ( <b>4</b> )	0	0-D	44	$\text{Rb}_3\text{VF}_6$ , $\text{Li}_6\text{WO}_6$	27, 57

<sup>a</sup> Counterions with different values of  $a$  have been incorporated.

$n$  of  $\text{A}_n\text{X}$  employed in reaction (1) increases while the connectedness (conn.) and, less rigorously, the dimensionality (dim.) decrease. Overall, there are 134 child compounds in accord with dimensional reduction distributed among 17 different framework types.

#### 4.2. Frameworks with Edge-Sharing Octahedra.

As the binding forces in a solid become more covalent, the Madelung term in the stabilization energy decreases in significance, while orienting atoms so as to optimize orbital overlap gains importance. The preference for corner-sharing structures is then commonly abandoned in favor of higher modes of connectivity. Relatedly, the tendency toward high metal coordination numbers diminishes and more structures exhibit tetrahedral coordination of the metal, where four highly directional orbitals are better suited to covalent bonding.<sup>32ab,39,58</sup> In addition, certain covalent structure types seem to differ only minimally in energy, as exemplified by the polymorphic compounds  $\text{TiCl}_3$ ,  $\text{TiBr}_3$ ,  $\text{ZrCl}_3$ , and  $\text{RuCl}_3$ , which can all adopt structures either with sheets of edge-sharing octahedra (as in **5**) or with chains of face-sharing octahedra.<sup>59</sup> As a result of these influences, many of the 164 binary compounds exhibiting structures with edge-sharing octahedra proceed to form child compounds with face-sharing octahedra or molecular tetrahedra. All told, 40% (91/226) of the ternary compounds in this class are consistent with dimensional reduction.

The most common binary structure with edge-sharing octahedra occurs in layered  $\text{MX}_2$  compounds with the  $\text{CdCl}_2$  or  $\text{CdI}_2$  structure types.<sup>24,60a</sup> Note that the stacking sequence of the  $\text{MX}_2$  sheets, which distinguishes between these two structure types, is not important for dimensional reduction. Table 3 enumerates the known child frameworks that arise from dimensional reduction of such parent compounds. Therein, ordered inverse spinels ( $\text{A}_2\text{MX}_4$ ) are differentiated from disordered inverse spinels; the former typically contain octahedra sharing only two edges to form four-connected chains, whereas the latter link octahedra through an average of two edges but have undetermined local variations. Among a total of 65 child compounds, only 8 distinct frameworks have been discovered thus far.

**Table 3. Frameworks Derived from MX<sub>2</sub> Compounds with Edge-Sharing Octahedra**

formula	conn.	dim.	no.	examples	ref
MX <sub>2</sub>	12	2-D	12	CdCl <sub>2</sub> , CdI <sub>2</sub> , SnS <sub>2</sub>	24, 60
AM <sub>4</sub> X <sub>9</sub>	11	3-D	1	CsMn <sub>4</sub> Cl <sub>9</sub>	61
A <sub>2</sub> M <sub>3</sub> X <sub>8</sub> ( <b>13</b> )	8	2-D	2	Na <sub>2</sub> Mn <sub>3</sub> Cl <sub>8</sub>	62
AMX <sub>3</sub> ( <b>6</b> )	8	1-D	30	KFeCl <sub>3</sub> , SnZrS <sub>3</sub>	63
A <sub>a</sub> MX <sub>3</sub> <sup>a</sup> ( <b>5</b> )	6	2-D	3	NaMnCl <sub>3</sub> , Na <sub>2</sub> ZrS <sub>3</sub>	21, 64
A <sub>2</sub> MX <sub>4</sub> ( <b>14</b> )	4	1-D	9	Na <sub>2</sub> MnCl <sub>4</sub>	65
A <sub>2</sub> MX <sub>4</sub> <sup>b</sup>			5	Li <sub>2</sub> VCl <sub>4</sub> , Li <sub>2</sub> FeCl <sub>4</sub>	66
A <sub>4</sub> M <sub>3</sub> X <sub>12</sub> :A <sub>2</sub> X <sub>3</sub>	4	1-D	2	La <sub>2</sub> SnS <sub>5</sub>	67
A <sub>4</sub> MX <sub>6</sub> ( <b>4</b> )	0	0-D	13	Na <sub>6</sub> MnCl <sub>8</sub> , Tl <sub>4</sub> CrI <sub>6</sub>	62, 68

<sup>a</sup> Counterions with different values of *a* have been incorporated.

<sup>b</sup> Disordered inverse spinel with mostly edge-sharing connectivity.

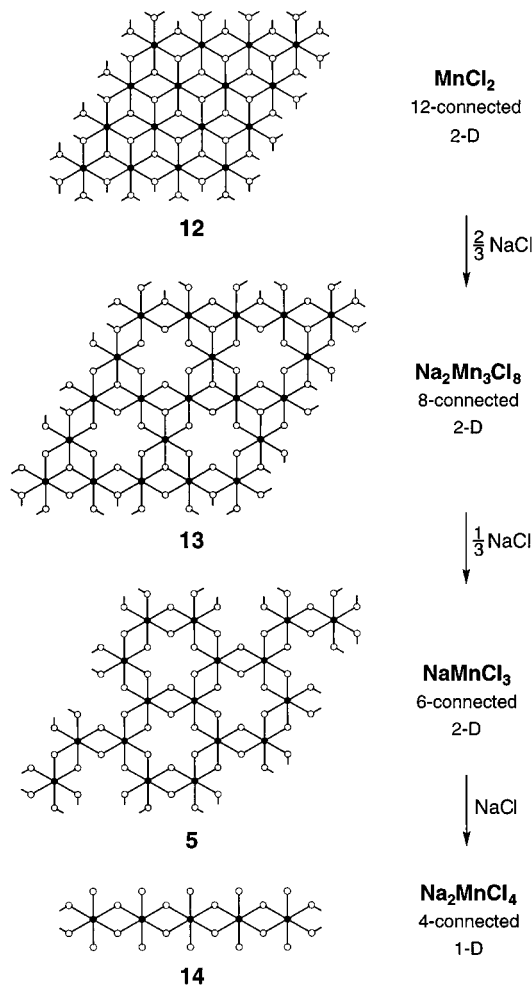


**Figure 7.** Deconstruction of a framework of edge-sharing octahedra. The two-dimensional, twelve-connected framework **12** incorporates additional anions to give less tightly connected sheets **13** and **5**. Further dimensional reduction yields the chain structure **14** and then finally discrete octahedral ions (**4**, not shown). Note that reaction equivalents given are all per mole of Mn.

As shown in Figure 7, treatment of MnCl<sub>2</sub> with NaCl affords an extensive dimensional reduction series, sampling four of the eight frameworks. The MnCl<sub>2</sub> parent compound adopts the CdCl<sub>2</sub> structure, with MnCl<sub>6</sub> octahedra sharing six edges to form twelve-connected sheets (**12**).<sup>23</sup> Reaction with two-thirds equivalents of NaCl yields Na<sub>2</sub>Mn<sub>3</sub>Cl<sub>8</sub> (=Na<sub>0.67</sub>MnCl<sub>2.67</sub>)<sup>62</sup> in which the added chloride ions produce eight-connected sheets with octahedra sharing just four edges (**13**). Another one-third equivalents of NaCl yields NaMnCl<sub>3</sub>, which ex-

**Table 4. Effects of the Counterion A on Compounds Derived from MX<sub>2</sub> Parent Frameworks with Edge-Sharing Octahedra**

child compound	cation, A <sup>+</sup>						
	Li	Na	In	K	Tl	Rb	Cs
<b>AMX<sub>3</sub></b>							
edge-sharing	1	1	3	6	7	3	1
face-sharing	0	0	0	1	5	11	18
<b>A<sub>2</sub>MX<sub>4</sub></b>							
edge-sharing	7	3		0		0	0
tetrahedral M	2	2		3		4	10

hibits a six-connected two-dimensional framework with octahedra sharing three edges (**5**).<sup>21</sup> Incorporating one more equivalent of NaCl yields Na<sub>2</sub>MnCl<sub>4</sub>, featuring chains of four-connected edge-sharing octahedra (**14**).<sup>65</sup> Notice how frameworks **13**, **5**, and **14** can be obtained from the structure of **12** by removing one-fourth, one-third, or one-half of the metal centers, respectively. Finally, excess NaCl extracts a saturated compound, with discrete octahedral [MnCl<sub>6</sub>]<sup>4-</sup> ions (**4**), as in Na<sub>6</sub>MnCl<sub>8</sub> (=Na<sub>4</sub>MnCl<sub>6</sub>·2NaCl).<sup>62</sup> It should be mentioned that since these are thermodynamic products from high-temperature solid-state reactions, it is not necessary to proceed with a synthesis in the stepwise fashion suggested by Figure 7; rather, each child compound can be prepared directly from a stoichiometric reaction between the parent compound and the dimensional reduction agent (reaction (1)).

Although the counterions A lie outside the M–X framework, they can still play a role in determining whether a specific system will follow the predictions of dimensional reduction. This is demonstrated in child compounds AMX<sub>3</sub> and A<sub>2</sub>MX<sub>4</sub> derived from the MX<sub>2</sub> (X = Cl, Br, I) parent framework **12** composed of edge-sharing octahedra. Table 4 summarizes the effect of varying the radius of the cation A<sup>+</sup> in these phases: clearly, dimensional reduction is much more reliable (i.e., more likely to result in a child framework with edge-sharing octahedra) here when a smaller, more polarizing cation is employed. This rule of thumb may extend to lower halides of transition metals in any oxidation state; however, there is not yet sufficient information in other systems to be certain. For example, all of the known unsaturated child compounds derived from MX<sub>3</sub> parents with edge-sharing octahedra contain face-sharing octahedra, but very few compounds with small counterions have been structurally characterized. If the effect of the counterion on the present class of compounds is general, then we can expect analogous phases incorporating smaller Li<sup>+</sup> or Na<sup>+</sup> cations to adopt structures with edge-sharing octahedra; this remains to be tested. For more on the role of the counterion A, see section 5.

#### 4.3. Frameworks with Face-Sharing Octahedra.

Eight binary metal halides adopt structures with MX<sub>3</sub> chains of face-sharing octahedra (**15**, see Figure 8). The structures of only four child compounds from these systems have been proven: Cs<sub>3</sub>Zr<sub>2</sub>I<sub>9</sub> and A<sub>3</sub>Mo<sub>2</sub>Br<sub>9</sub> (A = K, Rb, Cs).<sup>69</sup> All four exhibit molecular structures consistent with dimensional reduction in which two MX<sub>6</sub> octahedra share a common face to form dinuclear [M<sub>2</sub>X<sub>9</sub>]<sup>3-</sup> clusters (**16**). Such confacial bioctahedra are also frequently encountered in ternary metal halide compounds that derive from parents with edge-sharing

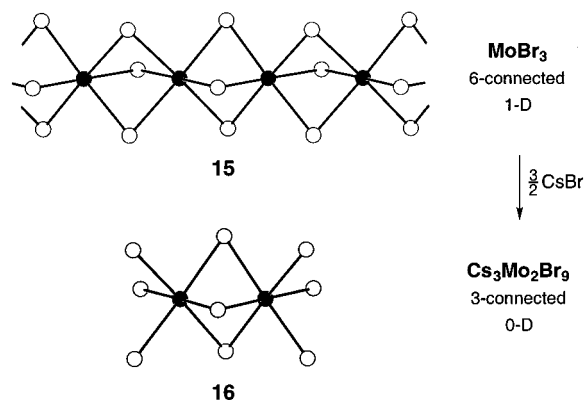


**Figure 8.** Terminating face-bridging interactions. MoBr<sub>3</sub> (top) has a one-dimensional, six-connected framework of face-sharing octahedra. Reaction with CsBr severs face-bridging interactions to yield discrete three-connected [Mo<sub>2</sub>Br<sub>9</sub>]<sup>3-</sup> conical bioctahedra in Cs<sub>3</sub>Mo<sub>2</sub>Br<sub>9</sub>.

octahedra and have been extensively studied with regard to the degree of bonding between metal centers.<sup>70</sup> Although the body of data here is extremely limited, it suggests that dimensional reduction provides a facile means of preparing these compounds. Further, dimensional reduction could potentially supply a convenient route to phases containing trinuclear [M<sub>3</sub>X<sub>12</sub>]<sup>3-</sup> (or longer) chain fragments of the type generated in solution and crystallized as (PPh<sub>4</sub>)<sub>3</sub>[Mo<sub>3</sub>I<sub>12</sub>].<sup>71</sup>

**4.4. Frameworks with Octahedra Linked by Mixed Connectivity Modes.** Many binary compounds exhibit structures with a mixture of connectivity modes. Foremost among these is the rutile structure (and the closely related CaCl<sub>2</sub> structure) in which octahedra share two trans edges to form chains, which are corner-bridged to form a twelve-connected three-dimensional framework.<sup>72</sup> This structure is adopted by relatively ionic compounds, including 10 fluorides and 3 lower halides of divalent metals, and 18 oxides of tetravalent metals. Dimensional reduction suggests that unsaturated child compounds in these systems should share corners and/or at most two edges, but does *not* predict which mode of connectivity will persist. Figure 9 shows two possible ways that incorporation of additional anions could lower the connectedness of a rutile-type framework. If incoming anions insert into M–X–M corner-sharing interactions, these corner bridges will be severed, resulting in a framework that retains the edge-sharing interactions. If incoming anions instead disrupt M–X–M linkages that are part of an edge-sharing interaction, the edge bridges convert into corner-sharing interactions. In nearly all binary compounds of this type, the M–X bonds belonging to edge-sharing interactions are longer than the M–X bonds involved in just corner-sharing interactions. The tendency for these perhaps weaker bonds to be severed preferentially upon dimensional reduction may account for the prevalence of corner-sharing structures in the ensuing ternary compounds.

As enumerated in Table 5, the 220 child compounds that derive from rutile-type parent compounds in accord with dimensional reduction—representing 58% of the 384 ternary phases structured—are distributed over 19 different frameworks. All but 29 of the unsaturated compounds adopt structures with strictly corner-sharing

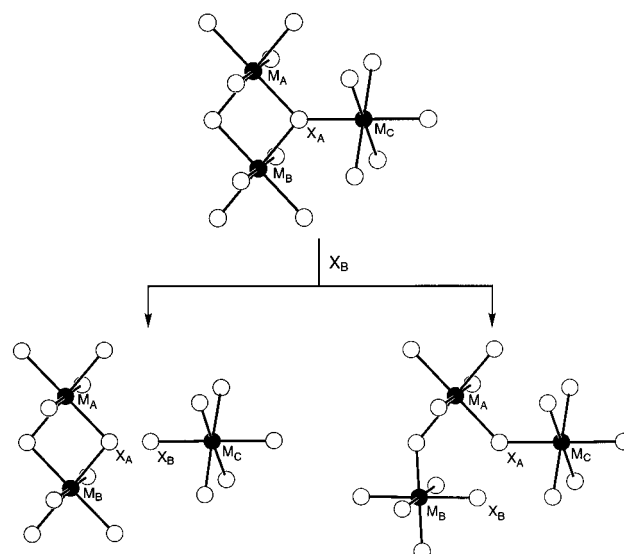


**Figure 9.** Inserting anions into the rutile structure. Upper: A portion of the rutile framework, with all anions equivalent, having  $\mu_3$  bonding as shown for X<sub>A</sub>. Left: Incorporating X<sub>B</sub> lowers the coordination number of X<sub>A</sub> by breaking the M<sub>C</sub>–X<sub>A</sub> bond, leaving an edge-sharing structure. Right: Incorporating X<sub>B</sub> again lowers the coordination number of X<sub>A</sub>, this time by inserting into the M<sub>B</sub>–X<sub>A</sub> bond, leaving a corner-sharing structure.

**Table 5. Frameworks Derived from MX<sub>2</sub> Compounds with a Rutile-Type Structure**

formula	conn.	dim.	no.	examples	ref
MX <sub>2</sub> ( <b>17</b> )	12	3-D	30	FeF <sub>2</sub> , TiO <sub>2</sub> , IrO <sub>2</sub>	72, 73
A <sub>2</sub> M <sub>5</sub> X <sub>14</sub> <sup>a</sup>	6.8	3-D	1	Ba <sub>2</sub> Cu <sub>5</sub> F <sub>14</sub>	74
AMX <sub>3</sub> ( <b>1</b> )	6	3-D	64	KMnF <sub>3</sub> , BaTiO <sub>3</sub>	75
A <sub>2</sub> M <sub>3</sub> X <sub>9</sub> <sup>a</sup> ·1/2A <sub>2</sub> X <sub>3</sub>	6	3-D	46	Y <sub>2</sub> Sn <sub>2</sub> O <sub>7</sub>	76
A <sub>2</sub> MX <sub>3</sub>	6	3-D	1	Li <sub>2</sub> ReO <sub>3</sub>	77
AMX <sub>3</sub> <sup>a</sup>	6	3-D	1	SrIrO <sub>3</sub>	78
AMX <sub>3</sub> ( <b>18</b> ) <sup>a</sup>	6	2-D	1	CaIrO <sub>3</sub>	79
A <sub>4</sub> M <sub>3</sub> X <sub>10</sub>	5.33	2-D	4	Sr <sub>4</sub> V <sub>3</sub> O <sub>10</sub>	80
A <sub>2</sub> M <sub>3</sub> X <sub>10</sub> <sup>a</sup>	5.33	3-D	2	Ba <sub>2</sub> Fe <sub>3</sub> F <sub>10</sub>	81
A <sub>3</sub> M <sub>2</sub> X <sub>7</sub>	5	2-D	20	K <sub>3</sub> Co <sub>2</sub> F <sub>7</sub> , Sr <sub>3</sub> Ti <sub>2</sub> O <sub>7</sub>	82
A <sub>2</sub> M <sub>2</sub> X <sub>7</sub>	5	2-D	3	La <sub>2</sub> Ti <sub>2</sub> O <sub>7</sub>	83
A <sub>2</sub> M <sub>2</sub> X <sub>7</sub> <sup>a</sup>	5	2-D	1	La <sub>2</sub> Mo <sub>2</sub> O <sub>7</sub>	84
A <sub>6</sub> M <sub>7</sub> X <sub>26</sub> <sup>a</sup>	4.86	3-D	3	Ba <sub>6</sub> Cu <sub>7</sub> F <sub>26</sub>	85
A <sub>2</sub> MX <sub>4</sub> <sup>b</sup> ( <b>2</b> )	4	2-D	35	K <sub>2</sub> NiF <sub>4</sub> , Sr <sub>2</sub> SnO <sub>4</sub>	86
A <sub>2</sub> MX <sub>4</sub> ( <b>14</b> ) <sup>a</sup>	4	1-D	12	Na <sub>2</sub> CrF <sub>4</sub> , Ca <sub>2</sub> IrO <sub>4</sub>	87
A <sub>2</sub> MX <sub>4</sub> <sup>a,c</sup>	4	1-D	7	Mg <sub>2</sub> MnO <sub>4</sub>	88
AMX <sub>4</sub>	4	2-D	6	BaMnF <sub>4</sub> , BaFeF <sub>4</sub>	89
A <sub>2</sub> MX <sub>4</sub> <sup>a</sup>	4	1-D	1	Pb <sub>2</sub> MnO <sub>4</sub>	90
A <sub>4</sub> M <sub>3</sub> X <sub>12</sub>	4	2-D	1	La <sub>4</sub> Ti <sub>3</sub> O <sub>12</sub>	91
A <sub>4</sub> MX <sub>6</sub> <sup>b</sup> ( <b>4</b> )	0	0-D	11	Ca <sub>4</sub> IrO <sub>6</sub> , Li <sub>8</sub> PtO <sub>6</sub>	92

<sup>a</sup> Framework retains edge-sharing interactions. <sup>b</sup> Counterions with different values of *a* have been incorporated. <sup>c</sup> Disordered inverse spinel with mostly edge-sharing connectivity.

connectivity. Thus, many of the frameworks listed here are also candidates for child compounds derived from MX<sub>3</sub> parents comprised of corner-sharing octahedra (and vice versa), albeit with different associated charges. Indeed, four of the frameworks, including **1**, **2**, and **4** (see Figure 1), are already common to both Tables 2 and 5. In contrast, the edge-sharing connectivity is only occasionally retained in rutile-based systems. An example where it does persist is depicted in Figure 10, with the dimensional reduction of IrO<sub>2</sub> (**17**)<sup>73b</sup> using CaO. Reaction with one equivalent of CaO lowers the coordination number of the oxide anions from three to two, generating six-connected sheets of IrO<sub>6</sub> octahedra

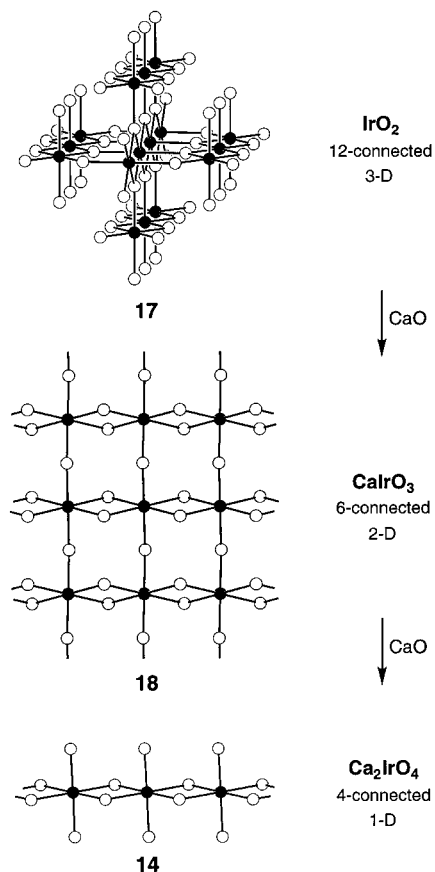


**Figure 10.** Dimensional reduction of a rutile framework with mixed connectivity modes. Incorporating CaO into  $\text{IrO}_2$  preserves edge-sharing interactions, while reducing the connectedness and dimensionality of the framework to yield sheets (**18**), chains (**14**), and discrete octahedral ions in  $\text{Ca}_4\text{IrO}_6$  (not shown). For clarity, outer bonds indicating the extended structure have been omitted from **17**.

sharing two edges and two corners (**18**) in  $\text{CaIrO}_3$ .<sup>79</sup> A second equivalent of CaO severs the corner-sharing interactions, yielding  $\text{Ca}_2\text{IrO}_4$ , with four-connected chains of octahedra sharing two edges (**14**).<sup>87</sup> Finally, an additional two equivalents is sufficient to terminate the remaining bridges and to form a saturated compound with discrete octahedral  $[\text{IrO}_6]^{8-}$  ions (**4**).<sup>92a</sup>

Thus, despite the lower metal oxidation states, the propensity for relatively ionic frameworks to assume structures with corner-sharing octahedra (as discussed in section 4.1) extends to the child compounds of  $\text{MX}_2$  phases with  $X = \text{O}, \text{F}$ . While the binary parent compounds might also be expected to adopt such structures, the presence of edge bridges can be rationalized with a simple geometric argument.<sup>93</sup> An  $\text{MX}_2$  framework exhibiting octahedral coordination of the metal centers must contain some anions with a coordination number of at least three.<sup>19</sup> As shown in Figure 11, for three regular octahedra to share a vertex while maintaining only corner-sharing interactions, the vertices on neighboring octahedra must come within close proximity of each other. In  $\text{PdS}_2$  and  $\beta\text{-HgO}_2$ , this is accommodated by forging a bond between anions,<sup>94</sup> while in  $\text{AgF}_2$ , the octahedra distort severely to give a 4 + 2 metal coordination.<sup>95</sup> However, most ionic  $\text{MX}_2$  solids instead adopt the rutile structure, accepting the less favorable edge-sharing interactions (with the concomitantly short-

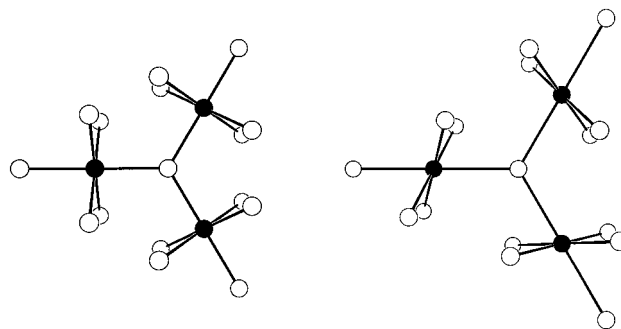


**Figure 11.** Geometric restrictions on corner-sharing octahedra. Left: Bringing three octahedrally coordinated metals together with only corner-bridging interactions forces anions from neighboring octahedra into very close contact. Right: Distortion of the coordination sphere around silver atoms in  $\text{AgF}_2$  separates these anions by lengthening the axial Ag–F bonds and tilting the equatorial plane.

ened metal–metal contacts) as a means of avoiding these anion–anion repulsions while maintaining approximately regular octahedral metal coordination. The mixture of connectivity modes is therefore due to geometric constraints associated with the very tightly connected framework necessitated by a low anion:metal ratio. Incorporating additional anions into the framework can release it from said constraints by eliminating the need for three-coordinate anions, permitting the child compound to adopt a structure with two-coordinate anions and the preferred corner-sharing of octahedra.

Mixed connectivity modes are found in many other condensed frameworks, including the commonly occurring nickel arsenide, corundum ( $\text{Al}_2\text{O}_3$ ), and  $C\text{-M}_2\text{O}_3$  (e.g.,  $\text{Mn}_2\text{O}_3$ ) structures.<sup>96</sup> As with descendants of the rutile structure, the less tightly connected child compounds derived from these structures usually tend toward adoption of a single persisting connectivity mode. Here again, a low anion:metal ratio coupled with the tendency to maximize metal coordination number, imposes high coordination numbers on the anions in the parent compound. This leads to utilization of less favored connectivity modes, which are then abandoned in the subsequent child compounds.

**4.5. Frameworks with Corner-Sharing Tetrahedra.** Numerous less ionic compounds, and particularly those with relatively small metal centers, assume structures composed of linked  $\text{MX}_4$  tetrahedra. In accord with Pauling's rules,<sup>38</sup> the tetrahedra typically share corners. Such frameworks are readily manipulated through dimensional reduction, with 272 of 416 ternary compounds (65%) displaying the expected structural characteristics. As enumerated in Table 6, nearly half of these derive from just seven  $\text{MX}_2$  parent compounds, each featuring a four-connected network of corner-sharing tetrahedra. A total of 19 distinct child frameworks are currently known, all but 3 of which are exemplified by silicon or germanium oxides. Note that, while there are many different structure types with two-connected chains of corner-sharing tetrahedra, all such known chains are topologically equivalent. This is contrary to the situation with two-connected chains of corner-sharing octahedra discussed in section 2 where cis–trans isomerism at individual metal centers can lead to variation in chain connectivity, as in frameworks **3** and **9** (see Figure 5).

**Table 6. Frameworks Derived from MX<sub>2</sub> Compounds with Corner-Sharing Tetrahedra**

formula	conn.	dim.	no.	examples	ref
MX <sub>2</sub>	4	3-D	8	BeF <sub>2</sub> , SiO <sub>2</sub> ( <b>19</b> )	97
A <sub>2</sub> M <sub>4</sub> X <sub>9</sub>	3.5	2-D	1	K <sub>2</sub> Si <sub>4</sub> O <sub>9</sub>	98
A <sub>6</sub> M <sub>10</sub> X <sub>23</sub>	3.4	3-D	1	Rb <sub>6</sub> Si <sub>10</sub> O <sub>23</sub>	99
A <sub>4</sub> M <sub>4</sub> X <sub>10</sub>	3	0-D	5	Na <sub>4</sub> Ge <sub>4</sub> S <sub>10</sub>	100
A <sub>2</sub> M <sub>2</sub> X <sub>5</sub> ( <b>20</b> )	3	2-D	4	Li <sub>2</sub> Si <sub>2</sub> O <sub>5</sub> , Li <sub>2</sub> Ge <sub>2</sub> O <sub>5</sub>	101
AM <sub>2</sub> X <sub>5</sub>	3	3-D	2	CsBe <sub>2</sub> F <sub>5</sub>	102
AM <sub>2</sub> X <sub>5</sub>	3	2-D	2	RbBe <sub>2</sub> F <sub>5</sub>	103
A <sub>2</sub> M <sub>2</sub> X <sub>5</sub>	3	2-D	2	Rb <sub>2</sub> Si <sub>2</sub> O <sub>5</sub>	101a
AM <sub>2</sub> X <sub>5</sub>	3	2-D	1	BaSi <sub>2</sub> O <sub>5</sub>	104
A <sub>3</sub> M <sub>5</sub> X <sub>13</sub>	2.8	1-D	1	Ba <sub>3</sub> Si <sub>5</sub> O <sub>13</sub>	105
A <sub>2</sub> M <sub>3</sub> X <sub>8</sub>	2.67	1-D	1	Ba <sub>2</sub> Si <sub>3</sub> O <sub>8</sub>	106
A <sub>8</sub> M <sub>5</sub> X <sub>14</sub>	2.4	0-D	1	Tl <sub>8</sub> Ge <sub>5</sub> O <sub>14</sub>	106
A <sub>a</sub> MX <sub>3</sub> ( <b>21</b> )	2	1-D	20	Li <sub>2</sub> SiO <sub>3</sub> , PbGeS <sub>3</sub>	107
A <sub>3a</sub> M <sub>3</sub> X <sub>9</sub> <sup>a</sup>	2	0-D	5	K <sub>6</sub> Si <sub>3</sub> O <sub>9</sub> , Sr <sub>3</sub> Ge <sub>3</sub> O <sub>9</sub>	108
A <sub>4</sub> M <sub>4</sub> X <sub>12</sub> ·4AX	2	0-D	1	Pb <sub>2</sub> SiO <sub>4</sub>	109
A <sub>3a</sub> M <sub>2</sub> X <sub>7</sub> <sup>a</sup> ( <b>22</b> )	1	0-D	28	Li <sub>6</sub> Si <sub>2</sub> O <sub>7</sub> , Na <sub>6</sub> Ge <sub>2</sub> S <sub>7</sub>	110
A <sub>4</sub> M <sub>4</sub> X <sub>14</sub>	1	0-D	3	La <sub>4</sub> Ge <sub>4</sub> O <sub>14</sub>	111
A <sub>5</sub> M <sub>3</sub> X <sub>11</sub>	0.67	0-D	2	Pb <sub>5</sub> Ge <sub>3</sub> O <sub>11</sub>	112
A <sub>5</sub> M <sub>3</sub> X <sub>11</sub> ·6AX	0.67	0-D	1	Pb <sub>11</sub> Si <sub>3</sub> O <sub>17</sub>	113
A <sub>2a</sub> MX <sub>4</sub> <sup>a</sup> ( <b>23</b> )	0	0-D	88	Li <sub>4</sub> SiO <sub>4</sub> , Mg <sub>2</sub> GeS <sub>4</sub>	114

<sup>a</sup> Counterions with different values of *a* have been incorporated.

The silicates represent by far the most thoroughly investigated of these systems. Their overwhelming preference for structures with corner-sharing tetrahedra is well documented,<sup>115</sup> so it comes as no surprise that dimensional reduction is extremely applicable to silicate frameworks. Indeed, it is probably here that the ideas of dimensional reduction are most deeply embedded in the mindset of solid-state chemists. Figure 12 depicts a dimensional reduction sequence relating some of the more common silicate frameworks with the incorporation of Li<sub>2</sub>O into the four-connected α-quartz structure of SiO<sub>2</sub> (**19**).<sup>97b</sup> Here, addition of successive one-half equivalents of Li<sub>2</sub>O produces compounds with frameworks of diminishing connectedness: corrugated three-connected sheets (**20**) in Li<sub>2</sub>Si<sub>2</sub>O<sub>5</sub>,<sup>101a</sup> two-connected chains (**21**) in Li<sub>2</sub>SiO<sub>3</sub>,<sup>107a</sup> discrete one-connected [Si<sub>2</sub>O<sub>7</sub>]<sup>6-</sup> anions (**22**) in Li<sub>6</sub>Si<sub>2</sub>O<sub>7</sub>,<sup>110a</sup> and finally, discrete molecular [SiO<sub>4</sub>]<sup>4-</sup> tetrahedra (**23**) in Li<sub>4</sub>SiO<sub>4</sub>.<sup>114a</sup> Dimensional reduction applies equally well to the frameworks in hundreds of quaternary silicates of the type A<sub>na</sub>A'<sub>i</sub>SiO<sub>x+n+i</sub>,<sup>93</sup> which are not included in our present study because they contain multiple counterions.

More condensed frameworks of corner-sharing tetrahedra are commonly observed in MX parent compounds that adopt the zinc blende<sup>116</sup> or wurtzite<sup>117</sup> structures. Note that the differences in overall connectivity between these two twelve-connected structures are of no consequence to the predictions of dimensional reduction. Of the 70 known ternary compounds stemming from parents of this type, 27 (39%) are in agreement with those predictions. As listed in Table 7, these child compounds exhibit six different framework types, three of which (**19**, **21**, and **23** in Figure 12) overlap with entries in Table 6.

#### 4.6. Frameworks with Edge-Sharing Tetrahedra.

Very few binary parent compounds favor structures with edge-sharing tetrahedra. Many alkali metal oxides and chalcogenides form A<sub>2</sub>X phases with the antifluorite structure, wherein AX<sub>4</sub> tetrahedra share all six edges; however, these are not appropriate as parent compounds for dimensional reduction. As shown in Figure 13, the structure of SiS<sub>2</sub> contains four-connected chains

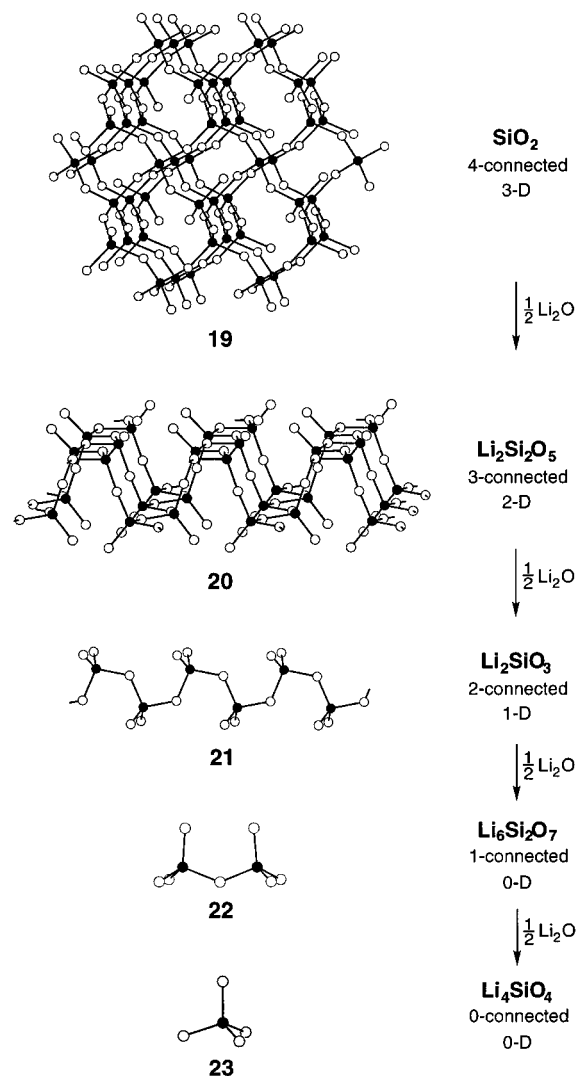


**Figure 12.** Dimensional reduction of SiO<sub>2</sub>, a parent structure composed of corner-sharing SiO<sub>4</sub> tetrahedra. At each step, reaction with successive one-half equivalents of Li<sub>2</sub>O (per mole of Si) reduces the connectedness of the framework by one. For clarity, outer bonds indicating the extended structure have been omitted from **19**.

**Table 7. Frameworks Derived from MX Compounds with Corner-Sharing Tetrahedra**

formula	conn.	dim.	no.	examples	ref
MX	12	3-D	20	CuCl, ZnO, ZnS	116–118
A <sub>4</sub> M <sub>3</sub> X <sub>5</sub>	6	2-D	1	Na <sub>4</sub> Cd <sub>3</sub> Se <sub>5</sub>	119
AMX <sub>2</sub>	4	2-D	2	SrZnO <sub>2</sub> , BaCdS <sub>2</sub>	120
AMX <sub>2</sub> ( <b>19</b> )	4	3-D	1	BaZnO <sub>2</sub>	121
A <sub>2</sub> M <sub>2</sub> X <sub>5</sub>	3	3-D	1	La <sub>2</sub> Be <sub>2</sub> O <sub>5</sub>	122
A <sub>2</sub> MX <sub>3</sub> ( <b>21</b> )	2	1-D	10	K <sub>2</sub> CuCl <sub>3</sub> , Ba <sub>2</sub> CdSe <sub>3</sub>	120b, 123
A <sub>6</sub> MX <sub>4</sub> ( <b>23</b> )	0	0-D	12	K <sub>6</sub> HgS <sub>4</sub> , Na <sub>6</sub> ZnO <sub>4</sub>	124

in which Si<sub>4</sub> tetrahedra share two opposite edges (**24**).<sup>125,126</sup> Reaction with one equivalent of Tl<sub>2</sub>S produces Tl<sub>4</sub>Si<sub>2</sub>S<sub>6</sub>, featuring two-connected [Si<sub>2</sub>S<sub>6</sub>]<sup>4-</sup> clusters in which two tetrahedra share a single common edge (**25**).<sup>127</sup> Incorporation of a second equivalent gives Tl<sub>4</sub>Si<sub>4</sub>S<sub>8</sub>, with isolated [Si<sub>4</sub>S<sub>8</sub>]<sup>4-</sup> tetrahedra.<sup>128</sup> In addition, several lower halides of group 13 metals form molecular M<sub>2</sub>X<sub>6</sub> complexes with the two-connected structure of **25**. Nearly all of the 37 structurally characterized ternary compounds arising in these systems possess saturated [MX<sub>4</sub>]<sup>-</sup> tetrahedra. The two known phases that do not

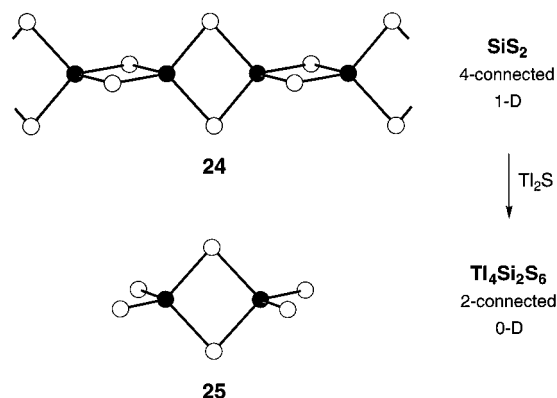


**Figure 13.** Dimensional reduction of  $\text{SiS}_2$ . Addition of successive equivalents of  $\text{Tl}_2\text{S}$  disrupts the one-dimensional chains of edge-sharing tetrahedra (**24**) to give dinuclear  $[\text{Si}_2\text{S}_6]^{4-}$  clusters (**25**) and mononuclear  $[\text{SiS}_4]^{4-}$  species (**23**, not shown).

are  $\text{KAl}_2\text{Br}_7$  and  $\text{KGa}_2\text{Cl}_7$ , which feature one-connected  $[\text{M}_2\text{X}_7]^-$  clusters with two tetrahedra sharing a corner (**22**);<sup>129</sup> in both cases, incorporation of additional  $\text{KX}$  leads to the expected saturated product.

**4.7. Frameworks with Other Metal Coordination Polyhedra.** Systems with less common metal coordination geometries can be quite amenable to dimensional reduction. Coordination geometries other than octahedral and tetrahedral often arise in a parent structure as a consequence of some electronic preference of the metal ion. Since dimensional reduction does not alter the electron count on the metal center, this preference will generally persist in the ensuing child compounds, contributing to the high degree of applicability of dimensional reduction in such systems. We shall look closely at two particular systems that typify the behavior observed in compounds with square planar coordination of  $d^8$  metals and linear coordination of certain  $d^{10}$  metals.

Along with four other binary metal oxides and chalcogenides in our database,  $\text{PdO}$  adopts the cooperite (PtS) structure type in which square planar  $\text{MX}_4$  units share two trans edges and four corners to form the three-dimensional network (**26**) shown in Figure 14.<sup>130</sup> Reaction with just one-third of an equivalent of  $\text{SrO}$  promptly disposes of all edge-sharing interactions, resulting in the corner-sharing three-dimensional framework (**27**) of  $\text{SrPd}_3\text{O}_4$ .<sup>131</sup> Incorporating additional  $\text{SrO}$  produces  $\text{Sr}_2\text{PdO}_3$ , featuring chains of coplanar square units sharing trans corners (**28**).<sup>131</sup> No compound achieving saturation with discrete  $[\text{PdO}_4]^{6-}$  anions has yet been structurally characterized. Dimensional reduction applies with similar success to most such systems; 81% (71/88) of all ternary compounds derived from parents with square planar metal coordination follow its predictions.

The compound  $\text{Cu}_2\text{O}$  exhibits a structure in which linearly coordinated  $\text{Cu}$  centers are linked through tetrahedrally coordinated oxide anions to give a three-dimensional framework analogous to that of  $\beta$ -cristobalite (**29**, Figure 15).<sup>132</sup> Two such frameworks actually interpenetrate in the crystal structure, but this does not affect the predictions of dimensional reduction. Reaction of  $\text{Cu}_2\text{O}$  with 0.6 equiv of  $\text{Rb}_2\text{O}$  generates  $\text{Rb}_3\text{Cu}_5\text{O}_4$ , which has a complicated two-dimensional net structure with linear  $\text{Cu}$  coordination (**30**).<sup>133</sup> Additional  $\text{Rb}_2\text{O}$

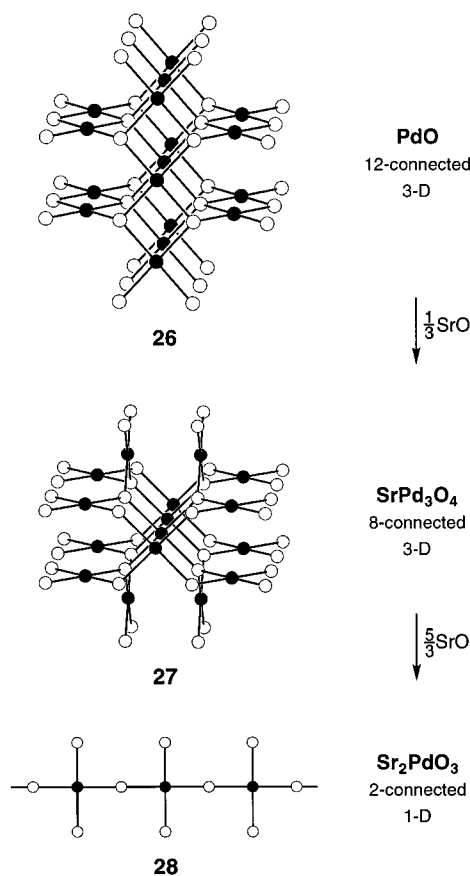


**Figure 14.** Deconstruction of a framework with square planar metal coordination. In  $\text{PdO}$ , square planar  $\text{PdO}_4$  units share two edges and four corners. Incorporation of  $\text{SrO}$  first severs all edge-bridging interactions to form **27** and then severs some corner-bridging interactions to form **28**. Note that reaction equivalents given are all per mole of  $\text{Pd}$ . For clarity, outer bonds indicating the extended structure have been omitted from **26** and **27**.

produces  $\text{Rb}_4\text{Cu}_4\text{O}_4$ , a compound containing molecular  $[\text{Cu}_4\text{O}_4]^{4-}$  squares (**31**).<sup>134</sup> The remaining bridges are cleaved upon assimilating one further equivalent of  $\text{Rb}_2\text{O}$  to form the saturated compound  $\text{Rb}_3\text{CuO}_2$ , with discrete linear  $[\text{CuO}_2]^{3-}$  ions (**32**).<sup>135</sup> As enumerated in Table 8, these and three other framework types are encountered among the 32 child compounds arising from  $\text{Cu}_2\text{O}$  and isostructural  $\text{Ag}_2\text{O}$ . With linear coordination, of course, higher connectivity modes are not possible, such that a child compound need only retain this metal coordination geometry to follow the predictions of dimensional reduction. And indeed, all 40 known ternary compounds derived from parent compounds with linear metal coordination do so.

**4.8. Saturated Compounds.** Thus far, we have focused our attention on the more complex structures of unsaturated compounds. However, dimensional reduction also provides an extremely effective method for preparing simple saturated compounds that are frequently of use in solution chemistry. For systems derived from parent compounds with linked octahedra, 92% (206/223) of all child compounds of the type  $A_n\text{M}\text{X}_{x+n}$  ( $x+n \geq 6$ ) do in fact contain the anticipated octahedral  $[\text{MX}_6]^{z-}$  anions. Similarly, for systems derived from linked tetrahedra, 97% (153/157) of all compounds of the type  $A_n\text{M}\text{X}_{x+n}$  ( $x+n \geq 4$ ) contain

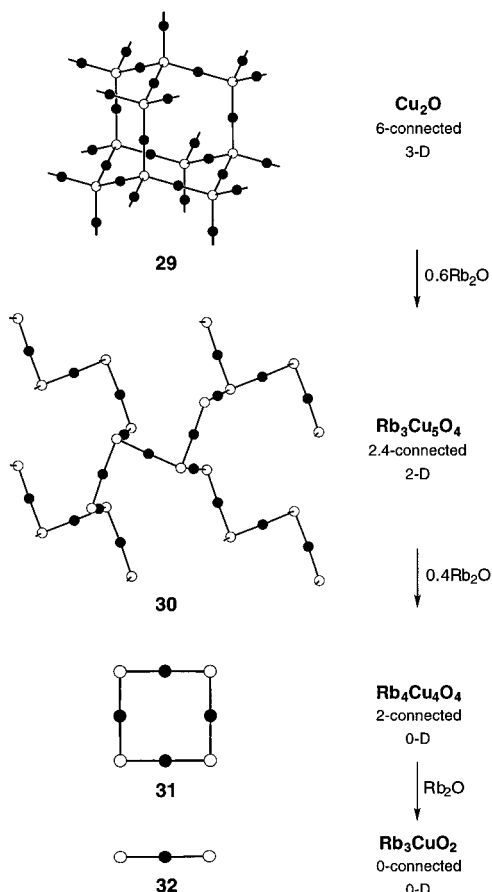


**Figure 15.** Dimensional reduction of  $\text{Cu}_2\text{O}$ , featuring a six-connected framework with linearly coordinated metal centers. Reaction with  $\text{Rb}_2\text{O}$  severs  $\text{Cu}-\text{O}-\text{Cu}$  linkages to form the two-dimensional framework **30**, the molecular square anion **31**, and finally the saturated  $[\text{CuO}_2]^{3-}$  anion **32**. Note that reaction equivalents given are all per mole of Cu.

**Table 8. Frameworks Derived from  $\text{M}_2\text{X}$  Compounds with Linear Metal Coordination**

formula	conn.	dim.	no.	examples	ref
$\text{M}_2\text{X}$ ( <b>29</b> )	6	3-D	2	$\text{Cu}_2\text{O}$ , $\text{Ag}_2\text{O}$	132, 136
$\text{AM}_3\text{X}_2$	4	3-D	2	$\text{LiAg}_3\text{O}_2$ , $\text{NaAg}_3\text{O}_2$	137
$\text{AM}_6\text{X}_4$	4	3-D	2	$\text{SrAg}_6\text{O}_4$ , $\text{BaAg}_6\text{O}_4$	138
$\text{A}_3\text{M}_5\text{X}_4$ ( <b>30</b> )	2.4	2-D	3	$\text{K}_3\text{Cu}_5\text{O}_4$ , $\text{Rb}_3\text{Cu}_5\text{O}_4$	133, 139
$\text{A}_4\text{M}_4\text{X}_4$ ( <b>31</b> )	2	0-D	8	$\text{Rb}_4\text{Cu}_4\text{O}_4$ , $\text{Na}_4\text{Ag}_4\text{O}_4$	134, 140
$\text{A}_a\text{MX}_2^a$	2	1-D	4	$\text{CsCuO}$ , $\text{PbAg}_2\text{O}_2$	141
$\text{A}_{3a}\text{MX}_2^a$ ( <b>32</b> )	0	0-D	13	$\text{Rb}_3\text{CuO}_2$ , $\text{Na}_3\text{AgO}_2$	135, 142

<sup>a</sup> Counterions with different values of  $a$  have been incorporated.

tetrahedral  $[\text{MX}_4]^{2-}$  anions. Multifarious solution-based techniques have been developed for synthesizing such molecular complexes. For example, the octahedral complex  $[\text{MoCl}_6]^{3-}$  has been prepared by a number of different methods, with varying degrees of difficulty and success. These methods, with reported yields ranging between 50 and 80%, include electrolytic reduction of  $\text{MoO}_3$  in concentrated HCl, oxidation of  $\text{Mo}_2(\text{O}_2\text{CCH}_3)_4$  in concentrated HCl, reduction of  $(\text{NH}_4)_6[\text{Mo}_7\text{O}_{24}] \cdot 4\text{H}_2\text{O}$  in concentrated HCl, and ligand substitution reactions of other  $\text{Mo}^{\text{III}}$  complexes.<sup>143</sup> Some of the syntheses are labor-intensive, but modifications or new approaches are sometimes difficult to devise since multiple species with varying ligand sets and metal oxidation states may be present in equilibrium. Yet dimensional reduction suggests a straightforward route to the desired product. A

solid-state reaction between the parent compound  $\text{MoCl}_3$  (**5**) and three equivalents of an alkali metal chloride dimensional reduction agent is expected to afford a soluble chiral compound  $\text{A}_3\text{MoCl}_6$  with molecular  $[\text{MoCl}_6]^{3-}$  anions. Indeed, we have found that  $\text{K}_3\text{MoCl}_6$  is formed in near quantitative yield by just such a reaction.<sup>144</sup> Often overlooked by solution chemists as a preparative method, dimensional reduction can offer a clean and efficient alternative means of synthesizing soluble molecular ions.

**4.9. Cluster-Containing Frameworks.** Solid phases containing early second and third row transition elements in low oxidation states sometimes exhibit multi-nuclear clusters—usually associated via metal–metal bonds—of generic type  $[\text{M}_m\text{Q}_q]$ , where Q represents an atom bonded to multiple metal centers within a cluster.<sup>145</sup> Such compounds have previously been excluded from our considerations; however, dimensional reduction can also be applied to frameworks composed of interlinked cluster units.<sup>16,146</sup> Take, for example, the binary phase  $\text{Mo}_6\text{Cl}_{12}$ , which adopts a two-dimensional structure featuring  $[\text{Mo}_6\text{Cl}_8]$  clusters.<sup>147</sup> The clusters possess a common  $[\text{M}_6\text{Q}_8]$  core geometry consisting of a central  $\text{M}_6$  octahedron with each triangular face capped by a  $\mu_3\text{-Q}$  atom. An additional ligand extends radially from each vertex of the octahedron, and it is through these outer ligands that intercluster bridging can occur. In  $\text{Mo}_6\text{Cl}_{12}$ , the outer ligands consist of two trans terminal Cl atoms and four bridging Cl atoms that link neighboring clusters to generate a four-connected sheet similar to **2** (see Figure 1), but with  $[\text{Mo}_6\text{Cl}_8]$  clusters positioned on the M atom sites. Reaction of  $\text{Mo}_6\text{Cl}_{12}$  with one equivalent of NaCl produces  $\text{NaMo}_6\text{Cl}_{13}$ ,<sup>148</sup> with two-connected chains of clusters similar to **3**, while reaction with two equivalents of CuCl produces  $\text{Cu}_2\text{Mo}_6\text{Cl}_{14}$ ,<sup>149</sup> containing discrete  $[\text{Mo}_6\text{Cl}_{14}]^{2-}$  molecules similar to **4**. Thus, incorporating additional anions can reduce the number of connections between cluster cores in a manner wholly analogous to the dimensional reduction of simple metal–anion frameworks.

The presence of Q atoms capable of serving as an outer ligand for a neighboring cluster permits a supplementary mode of connectivity between clusters—one that would correspond to direct bonding between metal atoms in our preceding treatment of metal–anion frameworks. This mode is exemplified in the structure of  $\text{Re}_6\text{Se}_8\text{Cl}_2$  (see Figure 16), wherein face-capped octahedral  $[\text{Re}_6\text{Se}_8]$  clusters, each with two trans terminal Cl ligands, are directly linked through intercluster  $\text{Re}-\text{Se}$  bonds to form eight-connected sheets (**33**).<sup>150</sup> The compact rhombic  $\text{Re}_2\text{Se}_2$  interactions connecting clusters render the framework intractable to low-temperature methods for excising molecular clusters.<sup>145b</sup> Dimensional reduction, however, can be employed as a means of disrupting intercluster bonds through insertion of intervening outer ligands. Thus, a high-temperature reaction incorporating one equivalent of TlCl yields  $\text{TlRe}_6\text{Se}_8\text{Cl}_3$ , in which each cluster unit now has three terminal chlorine ligands and is connected to only three neighboring clusters in a dimpled two-dimensional sheet (**34**).<sup>146</sup> Further incorporation of TlCl leads to the one-dimensional compound  $\text{Tl}_2\text{Re}_6\text{Se}_8\text{Cl}_4$ , with four terminal chlorine ligands and two trans bridging interactions per cluster (**35**), and finally, excess TlCl affords

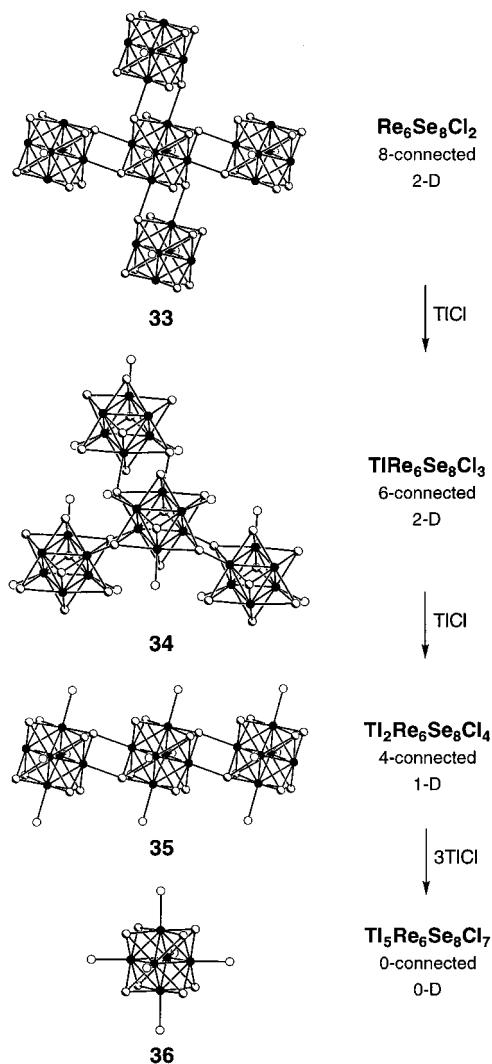


**Figure 16.** Dimensional reduction of  $\text{Re}_6\text{Se}_8\text{Cl}_2$  with  $\text{TiCl}$ . Only the local connectivity of a single cluster unit is depicted; black, shaded, and white spheres represent Re, Se, and Cl atoms, respectively. Each added equivalent of  $\text{TiCl}$  supplies another terminal chlorine ligand and destroys a rhombic  $\text{Re}_2\text{Se}_2$  interaction between clusters. For clarity, outer bonds indicating the extended structure have been omitted from **33**, **34**, and **35**.

$\text{Ti}_5\text{Re}_6\text{Se}_8\text{Cl}_7$  ( $=\text{Ti}_4\text{Re}_6\text{Se}_8\text{Cl}_6 \cdot \text{TiCl}$ ) with discrete  $[\text{Re}_6\text{Se}_8\text{Cl}_6]^{4-}$  clusters (**36**).<sup>146</sup> Related dimensional reduction reactions have provided this same cluster core in soluble form as  $\text{Cs}_4\text{Re}_6\text{Se}_8\text{I}_6$ ,<sup>16</sup> enabling access to a realm of previously unexplored solution chemistry.<sup>151</sup>

Cluster-containing solids that have been dismantled to some extent through dimensional reduction are enumerated in Table 9. Besides the face-capped octahedral  $[\text{M}_6\text{Q}_8]$  type clusters, many examples feature  $[\text{M}_6\text{Q}_{12}]$  clusters with a geometry consisting of an  $\text{M}_6$  octahedron that has each edge bridged by a  $\mu_2$ -Q atom and is sometimes centered by an interstitial atom. Another early example involves the extraction of edge-bridged triangular  $[\text{Re}_3\text{Cl}_3]$  clusters from  $\text{Re}_3\text{Cl}_9$ .<sup>178</sup> In many instances, this provides access to soluble molecular clusters for which there is no known method of assembly in solution. It is worth noting that the added complexity of the cluster units can provide additional avenues for adjusting the framework connectedness, including using a Q' constituent with a different formal

**Table 9. Dimensional Reduction of Cluster-Containing Solids**

parent phase	dim.	child compounds <sup>a</sup>	dim.	ref
<b>[M<sub>6</sub>Q<sub>8</sub>]-Type</b>				
$\text{Mo}_6\text{Cl}_{12}$	2-D	$\text{NaMo}_6\text{Cl}_{13}$	1-D	147, 148
		$\text{Cu}_2\text{Mo}_6\text{Cl}_{14}$	0-D	149
$\text{Mo}_6\text{Br}_{12}$	2-D	$\text{Cs}_2\text{Mo}_6\text{Br}_{14}$	0-D	152
$\text{Mo}_6\text{I}_{12}$	2-D	$\text{PbMo}_6\text{I}_{14}$	0-D	153
$\text{W}_6\text{Br}_{12}$	2-D	$\text{K}_2\text{W}_6\text{Br}_{14}$	0-D	152b, 154
$\text{Li}_4\text{Re}_6\text{S}_{11}$	3-D	$\text{Rb}_{10}\text{Re}_6\text{S}_{14}$	0-D	155
$\text{Re}_6\text{S}_8\text{Cl}_2$	3-D	$\text{Ti}_2\text{Re}_6\text{S}_8\text{Cl}_4$	1-D	146, 156
		$\text{Cs}_5\text{Re}_6\text{S}_8\text{Cl}_7$	0-D	146
$\text{Re}_6\text{S}_5\text{Cl}_8$	1-D	$\text{RbRe}_6\text{S}_5\text{Cl}_9$	0-D	157
$\text{Re}_6\text{S}_8\text{Br}_2$	3-D	$\text{Cs}_5\text{Re}_6\text{S}_8\text{Br}_7$	0-D	16, 158
$\text{Re}_6\text{S}_7\text{Br}_4$	3-D	$\text{Rb}_3\text{Re}_6\text{S}_7\text{Br}_7$	0-D	159
$\text{Re}_6\text{Se}_8\text{Cl}_2$ ( <b>33</b> )	2-D	$\text{TiRe}_6\text{Se}_8\text{Cl}_3$ ( <b>34</b> )	2-D	146, 150
		$\text{Ti}_2\text{Re}_6\text{Se}_8\text{Cl}_4$ ( <b>35</b> )	1-D	146
		$\text{Ti}_5\text{Re}_6\text{Se}_8\text{Cl}_7$ ( <b>36</b> )	0-D	146
$\text{Re}_6\text{Se}_6\text{Cl}_6$	2-D	$\text{Cs}_2\text{Re}_6\text{Se}_6\text{Cl}_8$	0-D	160
$\text{Re}_6\text{Se}_5\text{Cl}_8$	1-D	$\text{KRe}_6\text{Se}_5\text{Cl}_9$	0-D	159a, 161
$\text{Re}_6\text{Se}_8\text{Br}_2$	3-D	$\text{Cs}_2\text{Re}_6\text{Se}_8\text{Br}_4$	1-D	16, 162
$\text{CsRe}_6\text{Se}_8\text{I}_3$	2-D	$\text{Cs}_4\text{Re}_6\text{Se}_8\text{I}_6$	0-D	16
<b>[M<sub>6</sub>Q<sub>12</sub>]-Type</b>				
$\text{Zr}_6\text{HCl}_{12}$	3-D	$\text{Li}_6\text{Zr}_6\text{HCl}_{18}$	0-D	163
$\text{Zr}_6\text{BeCl}_{12}$	3-D	$\text{KZr}_6\text{BeCl}_{13}$	3-D	163a, 164
		$\text{K}_3\text{Zr}_6\text{BeCl}_{15}$	3-D	165
		$\text{Na}_4\text{Zr}_6\text{BeCl}_{16}$	2-D	166
		$\text{Ba}_3\text{Zr}_6\text{BeCl}_{18}$	0-D	167
$\text{Zr}_6\text{BCl}_{13}^b$	3-D	$\text{RbZr}_6\text{BCl}_{14}$	3-D	163a, 168
		$\text{K}_2\text{Zr}_6\text{BCl}_{15}$	3-D	165
		$\text{Rb}_2\text{Zr}_6\text{BCl}_{15}$	3-D	169
		$\text{Cs}_3\text{Zr}_6\text{BCl}_{16}$	2-D	166
		$\text{Ba}_2\text{Zr}_6\text{BCl}_{17}$	1-D	170
		$\text{Rb}_5\text{Zr}_6\text{BCl}_{18}$	0-D	171
$\text{Zr}_6\text{CCl}_{14}$	3-D	$\text{KZr}_6\text{CCl}_{15}$	3-D	163a, 169
		$\text{Rb}_4\text{Zr}_6\text{CCl}_{18}$	0-D	172
$\text{LiZr}_6\text{MnCl}_{14}$	3-D	$\text{Li}_2\text{Zr}_6\text{MnCl}_{15}$	3-D	173
$\text{Zr}_6\text{FeCl}_{14}$	3-D	$\text{CsZr}_6\text{FeCl}_{15}$	3-D	169, 173a
$\text{Zr}_6\text{FeBr}_{14}$	3-D	$\text{CsZr}_6\text{FeBr}_{15}$	3-D	169, 174
$\text{Nb}_6\text{Cl}_{14}$	3-D	$\text{LiNb}_6\text{Cl}_{15}$	3-D	175
		$\text{Li}_2\text{Nb}_6\text{Cl}_{16}$	2-D	176
		$\text{K}_4\text{Nb}_6\text{Cl}_{18}$	0-D	177
<b>Other Types</b>				
$\text{Re}_3\text{Cl}_9$	2-D	$\text{Cs}_3\text{Re}_3\text{Cl}_{12}$	0-D	178
$\text{Re}_3\text{Br}_9$	2-D	$\text{RbRe}_3\text{Br}_{10}$	1-D	179

<sup>a</sup> A selected example is given for each known framework type.

<sup>b</sup> This compound features an additional type of connectivity mode in which neighboring cluster cores share a common Q atom.

charge or altering the electron count associated with an interstitial or heterometal atom.

## 5. Applying Dimensional Reduction

Using dimensional reduction to target a specific framework is a relatively uncomplicated task. A standard high-temperature reaction between the parent solid and a stoichiometric amount of the dimensional reduction agent will usually suffice to provide a child compound with the desired characteristics.<sup>180</sup> Indeed, with only a few exceptions, all ternary compounds used as examples in the text have been produced in this manner. Certain systems, however, can be difficult to manipulate with some counteractions, as observed in section 4.2 with the incorporation of larger cations in the lower halides of transition metals. Such a dependence on cation size is by no means unique to these compounds. In fact, the success of dimensional reduction has been proven to depend on the choice of cation in roughly one-third of all compounds considered.<sup>181</sup> Restricting our data to these cation-dependent systems,

the applicability of dimensional reduction steadily decreases from A = lithium (64%) to cesium (14%) and from A = beryllium (100%) to barium (40%), in agreement with our prior observations in Table 4. Earlier, it was assumed that the metal–anion interaction changes little as the result of a dimensional reduction reaction; here, we must examine the validity of that assumption. Terminal anions will possess more electron density than bridging anions since the electrons are shared with fewer positively charged metal centers (which provides the basis for their heightened electrostatic bond strength in Pauling's rules).<sup>38</sup> As dimensional reduction lowers the coordination number of the anions, they become effectively larger and more negatively charged, in many cases leading to reduction of the metal coordination number. The more highly charged terminal anions are attractive to cations, so it is here that our assumption of noninteraction with the counterion is challenged. If the cation is strongly polarizing (i.e., small and highly charged), then it will draw electron density away from the anion, countering any increase in effective size and charge of the anion with respect to a metal center in the framework. Such mitigating effects will not be in operation under the influence of a weakly polarizing cation. Thus, in many cases, the use of a small, highly charged counterion A will help minimize the increase of electron density on the anions, extending the success of dimensional reduction.

In cases where a direct synthesis cannot be accomplished, ternary compounds with larger counterions can still potentially be accessed through dimensional reduction by taking advantage of the kinetic stability of the framework. If the desired framework is open and can be produced with some smaller cation by dimensional reduction, it may subsequently be possible to carry out a cation exchange reaction using a low-temperature technique<sup>10</sup> without perturbing the framework. Of the ternary compounds that adopt structures inconsistent with dimensional reduction, nearly one-third has a known analogue, formally related through cation exchange, which does exhibit the predicted structural characteristics. Thus, if a specific cation–framework combination is required, it is advisable to attempt suitable dimensional reduction reactions with a variety of different cations, followed, if necessary, by an ion exchange reaction. In this way, dimensional reduction can be coupled with other synthetic methods to provide access to a wider range of solids.

Aside from its general utility in the synthesis of new solids, dimensional reduction is particularly well-suited for preparing compounds in which a physical property inherent to the known parent compound is dimensionally restricted. Indeed, many physical properties that arise largely from through-bond phenomena are readily manipulated with dimensional reduction. As an example, consider the electronic structures for the series of frameworks depicted in Figure 1. In the tightly connected parent structure **1**, a conduction band electron is easily delocalized across the framework. As connections in the framework are severed, the spread of the band narrows until the saturated compound **4** contains isolated ions without covalent linkages; here, electrons should be quite localized and conductivity is expected to be poor. Between these two extremes,

frameworks **2** and **3** may exhibit anisotropic conductivity within the sheets or along the chains, respectively. In contrast, one could envision an opposing trend in ionic conductivity, as propagated through the cations A and confined by the framework. Other properties of inorganic solids that rely primarily on connections between metal centers and local geometrical parameters that are conserved by dimensional reduction should be similarly adjustable. Thus, the study of materials of interest for their mechanical, optical, magnetic, and thermoelectric properties may also be facilitated by dimensional reduction.

Dimensional reduction additionally provides a straightforward empirically derived means for predicting certain facets of the structure of an unknown compound. A ternary compound is easily traced back to its binary parent, the structure of which then supplies information concerning the child framework. For example, an unknown compound of formula NaCoF<sub>4</sub> is traced back to CoF<sub>3</sub> by extracting one equivalent of NaF. Since the structure of CoF<sub>3</sub> exhibits CoF<sub>6</sub> octahedra sharing all six corners (**1**),<sup>182</sup> the child compound NaCoF<sub>4</sub> is expected to possess a four-connected framework of corner-sharing octahedra. While this does not pinpoint a specific crystal structure, it significantly restricts the list of likely candidates (see Table 2) from which the structure type might be recognized by comparing X-ray powder diffraction patterns. A wide range of compounds have the composition AMX<sub>4</sub>, yet dimensional reduction applies to all of these systems with some degree of success, describing 68% where X = F, 59% where X = Cl, 73% where X = Br, 100% where X = I, and 21% where X = O. Note that this method is readily applied to any ternary composition, without requiring extensive calculations.

## 6. Summary and Outlook

An important aspect of the recent development of solid-state chemistry has been the recognition of new synthetic techniques that permit some control over the ensuing product structure. Herein, we formalize and systematically evaluate an enduring method for dismantling binary metal–anion (M–X) frameworks composed of linked metal-centered polyhedra. In essence, dimensional reduction reactions sever connections between neighboring polyhedra in such a framework by incorporating additional bridge-terminating anions into the compound. Electropositive cations A are used to balance charge, without influencing the covalent M–X framework. The metal coordination geometry and polyhedron connectivity mode of the parent structure are retained in the framework of the ensuing ternary phase, enabling prediction of its connectedness—defined as the mean number of distinct M–X–M linkages around the metal centers. The scope of this reaction type can be assessed through examination of a database containing 2497 ternary structures derived from 524 binary compounds. Solids with octahedral, tetrahedral, square planar, and linear metal coordination geometries linked through a variety of connectivity modes are amenable to dimensional reduction, lending this approach widespread utility. In targeting a specific subsidiary framework, the choice of A should be viewed as an experimental variable, with smaller cations generally providing more consistent results.





- (121) von Schnering, H. G.; Hoppe, R.; Zemann, J. *Z. Anorg. Allg. Chem.* **1960**, *305*, 241–254.
- (122) Harris, L. A.; Yakel, H. L. *Acta Crystallogr.* **1968**, *B24*, 672–682.
- (123) Brink, C.; MacGillavry, C. H. *Acta Crystallogr.* **1949**, *2*, 158–163.
- (124) (a) Sommer, H.; Hoppe, R.; Jansen, M. *Naturwissenschaften* **1976**, *63*, 194–195. (b) Kastner, P.; Hoppe, R. *Z. Anorg. Allg. Chem.* **1974**, *409*, 69–76.
- (125) Peters, J.; Krebs, B. *Acta Crystallogr.* **1982**, *B38*, 1270–1272.
- (126) Only  $\text{BeCl}_2$  is known to have an analogous structure: Rundle, R. E.; Lewis, P. H. *J. Chem. Phys.* **1952**, *20*, 132–134.
- (127) Eulenberger, G. *Monatsh. Chem.* **1982**, *113*, 859–867.
- (128) Eulenberger, G. *Acta Crystallogr.* **1986**, *C42*, 528–534.
- (129) (a) Rytter, E.; Rytter, B. E. D.; Øye, H. A.; Krogh-Moe, J. *Acta Crystallogr.* **1973**, *B29*, 1541–1543. (b) Mascherpa-Corrall, D.; Vitse, P.; Potier, A.; Darriet, J. *Acta Crystallogr.* **1976**, *B32*, 247–250.
- (130) (a) Moore, W. J.; Pauling, L. *J. Am. Chem. Soc.* **1941**, *63*, 1392–1394. (b) Grønvald, F.; Haraldsen, H.; Kjekshus, A. *Acta Chem. Scand.* **1960**, *14*, 1879–1893.
- (131) Muller, O.; Roy, R. *Adv. Chem.* **1971**, *98*, 28–38.
- (132) Restori, R.; Schwarzenbach, D. *Acta Crystallogr.* **1986**, *B42*, 201–208.
- (133) Klassen, H.; Hoppe, R. *Z. Anorg. Allg. Chem.* **1982**, *494*, 20–30.
- (134) Losert, W.; Hoppe, R. *Z. Anorg. Allg. Chem.* **1985**, *524*, 7–16.
- (135) Carl, W.; Hoppe, R. *Naturwissenschaften* **1969**, *485*, 92–100.
- (136) Niggli, P. *Z. Kristallogr. Kristallgeom. Kristallphys. Kristallchem.* **1922**, *57*, 253–299.
- (137) (a) Jansen, M. *Z. Naturforsch.* **1975**, *B30*, 854–858. (b) Jansen, M. *Z. Naturforsch.* **1976**, *B31*, 1544.
- (138) (a) Keller, H.-L.; Müller-Buschbaum, H. *Z. Anorg. Allg. Chem.* **1972**, *393*, 266–274. (b) Keller, H.-L.; Müller-Buschbaum, H. *Z. Naturforsch.* **1973**, *B28*, 263–267.
- (139) Hoppe, R.; Losert, Z. *Z. Anorg. Allg. Chem.* **1983**, *504*, 60.
- (140) Fischer, D.; Carl, W.; Glaum, H.; Hoppe, R. *Z. Anorg. Allg. Chem.* **1990**, *585*, 75–81.
- (141) Jansen, M.; Bortz, M. *Z. Anorg. Allg. Chem.* **1989**, *579*, 123–128.
- (142) Klassen, H.; Hoppe, R. *Z. Anorg. Allg. Chem.* **1982**, *485*, 92–100.
- (143) (a) Hartmann, H.; Schmidt, H.-J. *Z. Phys. Chem. Neue Folge* **1957**, *11*, 234–250. (b) Brenčić, J. V.; Cotton, F. A. *Inorg. Synth.* **1972**, *13*, 170–173. (c) Shibahara, T.; Yamasaki, M. *Bull. Soc. Chem. Jpn.* **1990**, *63*, 3022–3023.
- (144) Heinrich, J. L.; Long, J. R. Unpublished results. The reactants were heated at 800 °C in a sealed, evacuated quartz tube for 3 days; product identity and purity were verified by X-ray powder diffraction.
- (145) (a) Simon, A. *Angew. Chem., Int. Ed. Engl.* **1988**, *27*, 159–183. (b) Lee, S. C.; Holm, R. H. *Angew. Chem., Int. Ed. Engl.* **1990**, *29*, 840–856, and references therein. (c) Simon, A.; Mattausch, H.; Miller, G. J.; Bauhoffer, W.; Kremer, R. K. *Handbook on the Physics and Chemistry of Rare Earths, Vol. 15*; Gschneider, K. A., Jr., Eyring, L., Eds.; North-Holland Pub. Co.: New York, 1991; pp 191–285. (d) Hughbanks, T. *J. Alloys Compd.* **1995**, *229*, 40–53. (e) Corbett, J. D. *J. Chem. Soc., Dalton Trans.* **1996**, 575–587. (f) Saito, T. *J. Chem. Soc., Dalton Trans.* **1999**, 97–105.
- (146) Long, J. R.; Williamson, A. S.; Holm, R. H. *Angew. Chem., Int. Ed. Engl.* **1995**, *34*, 226–229.
- (147) von Schnering, H. G.; May, W.; Peters, K. *Z. Kristallogr.* **1993**, *208*, 368–369.
- (148) Boesch, S.; Keller, H. L. *Z. Kristallogr.* **1991**, *196*, 159–168.
- (149) Peppenhorst, A.; Keller, H.-L. *Z. Anorg. Allg. Chem.* **1996**, *622*, 663–669.
- (150) Leduc, L.; Perrin, A.; Sergent, M. *Acta Crystallogr.* **1983**, *C39*, 1503–1506.
- (151) (a) Zheng, Z.; Long, J. R.; Holm, R. H. *J. Am. Chem. Soc.* **1997**, *119*, 2163–2171. (b) Zheng, Z.; Holm, R. H. *Inorg. Chem.* **1997**, *36*, 5173–5178. (c) Beauvais, L. G.; Shores, M. P.; Long, J. R. *Chem. Mater.* **1998**, *10*, 3783–3786. (d) Shores, M. P.; Beauvais, L. G.; Long, J. R. *J. Am. Chem. Soc.* **1999**, *121*, 775–779. (e) Wang, R.; Zheng, Z. *J. Am. Chem. Soc.* **1999**, *121*, 3549–3550. (f) Zheng, Z.; Gray, T. G.; Holm, R. H. *Inorg. Chem.* **1999**, *38*, 4888–4895. (g) Gray, T. G.; Rudzinski, C. M.; Nocera, D. G.; Holm, R. H. *Inorg. Chem.* **1999**, *38*, 5932–5933. (h) Beauvais, L. G.; Shores, M. P.; Long, J. R. *J. Am. Chem. Soc.* **2000**, *122*, 2763–2772. (i) Bennett, M. V.; Shores, M. P.; Beauvais, L. G.; Long, J. R. *J. Am. Chem. Soc.* **2000**, *122*, 6664–6668.
- (152) (a) Zheng, Y.-Q.; Peters, K.; Hönle, W.; Grin, Y.; von Schnering, H. G. *Z. Kristallogr.* **1997**, *212*, 453–457. (b) Zheng, Y.-Q.; Peters, K.; Grin, Y.; von Schnering, H. G. *Z. Anorg. Allg. Chem.* **1998**, *624*, 506–512.
- (153) (a) Aliev, Z. G.; Klinkova, L. A.; Dubrovin, I. V.; Atovnyan, L. O. *Zh. Neorg. Khim.* **1981**, *26*, 1964–1967. (b) Boesch, S.; Keller, H. L. *Z. Kristallogr.* **1992**, *200*, 305–315.
- (154) Sassmannshausen, J.; von Schnering, H. G. *Z. Anorg. Allg. Chem.* **1994**, *620*, 1312–1320.
- (155) (a) Bronger, W.; Miessen, H. J.; Müller, P.; Neugroschel, R. *J. Less-Common Met.* **1985**, *105*, 303–310. (b) Bronger, W.; Kanert, M.; Loevenich, M.; Schmitz, D. *Z. Anorg. Allg. Chem.* **1993**, *619*, 2015–2020.
- (156) Fischer, C.; Fiechter, S.; Tributsch, H.; Reck, G.; Schultz, B. *Ber. Bunsen-Ges. Phys. Chem.* **1992**, *96*, 1652–1658.
- (157) Gabriel, J.-C.; Boubekeur, K.; Batail, P. *Inorg. Chem.* **1993**, *32*, 2894–2900.
- (158) Fischer, C.; Alonso-Vante, N.; Fiechter, S.; Tributsch, H.; Reck, G.; Schulz, W. *J. Alloys Compd.* **1992**, *178*, 305–314.
- (159) (a) Perrin, A.; Leduc, L.; Sergent, M. *Eur. J. Solid State Inorg. Chem.* **1991**, *28*, 919–931. (b) Slougui, A.; Perrin, A.; Sergent, M. *J. Solid State Chem.* **1999**, *147*, 358–365.
- (160) Leduc, L.; Perrin, A.; Sergent, M. *C. R. Acad. Sci. Ser. 2* **1983**, *296*, 961–966.
- (161) Perrin, A.; Leduc, L.; Potel, M.; Sergent, M. *Mater. Res. Bull.* **1990**, *25*, 1227–1234.
- (162) Speziali, N. L.; Berger, H.; Leicht, G.; Sanjinés, R.; Chapuis, G.; Lévy, F. *Mater. Res. Bull.* **1988**, *23*, 1597–1604.
- (163) (a) Ziebarth, R. P.; Corbett, J. D. *J. Solid State Chem.* **1989**, *80*, 56–67. (b) Zhang, J.; Ziebarth, R. P.; Corbett, J. D. *Inorg. Chem.* **1992**, *31*, 614–619.
- (164) Ziebarth, R. P.; Corbett, J. D. *Acc. Chem. Res.* **1989**, *22*, 256–262.
- (165) Ziebarth, R. P.; Corbett, J. D. *J. Am. Chem. Soc.* **1988**, *110*, 1132–1139.
- (166) Ziebarth, R. P.; Corbett, J. D. *Inorg. Chem.* **1989**, *28*, 626–631.
- (167) Zhang, J.; Corbett, J. D. *Z. Anorg. Allg. Chem.* **1991**, *598/599*, 363–370.
- (168) Kockerling, M.; Qi, R. Y.; Corbett, J. D. *Inorg. Chem.* **1996**, *35*, 1437–1443.
- (169) Ziebarth, R. P.; Corbett, J. D. *J. Am. Chem. Soc.* **1987**, *109*, 4844–4850.
- (170) Zhang, J.; Corbett, J. D. *J. Less-Common Met.* **1989**, *156*, 49–58.
- (171) Ziebarth, R. P.; Corbett, J. D. *J. Am. Chem. Soc.* **1989**, *111*, 3272–3280.
- (172) Zhang, J.; Ziebarth, R. P.; Corbett, J. D. *Inorg. Chem.* **1992**, *31*, 614–619.
- (173) (a) Zhang, J.; Corbett, J. D. *J. Solid State Chem.* **1994**, *109*, 265–271. (b) Zhang, J.; Corbett, J. D. *Inorg. Chem.* **1991**, *30*, 431–435.
- (174) Hughbanks, T.; Rosenthal, G.; Corbett, J. D. *J. Am. Chem. Soc.* **1986**, *108*, 8289–8290.
- (175) (a) Simon, A.; von Schnering, H.-G.; Wöhrle, H.; Schäfer, H. *Z. Anorg. Allg. Chem.* **1965**, *339*, 155–170. (b) Bajan, B.; Balzer, G.; Meyer, H.-J. *Z. Anorg. Allg. Chem.* **1997**, *623*, 1723–1728.
- (176) Bajan, B.; Meyer, H.-J. *Z. Anorg. Allg. Chem.* **1997**, *623*, 791–795.
- (177) Simon, A.; von Schnering, H.-G.; Schaefer, H. *Z. Anorg. Allg. Chem.* **1968**, *361*, 235–246.
- (178) (a) Cotton, F. A.; Mague, H. T. *Inorg. Chem.* **1964**, *3*, 1402. (b) Meyer, G.; Irmiler, M. *J. Less-Common Met.* **1986**, *119*, 31–44.
- (179) (a) Cotton, F. A.; Lippard, S. J.; Mague, J. T. *Inorg. Chem.* **1965**, *4*, 508–514. (b) Jung, B.; Meyer, G. *Z. Anorg. Allg. Chem.* **1991**, *597*, 107–113.
- (180) (a) West, A. R. *Solid State Chemistry and Its Applications*; John Wiley & Sons: New York, 1984; pp 4–46. (b) *Solid State Chemistry Techniques*; Cheetham, A. K., Day, P., Eds.; Oxford University Press: New York, 1987; pp 1–38.
- (181) That is, one in every three compounds,  $\text{A}_{na}\text{MX}_{x+n}$ , has a known sibling compound,  $\text{A}_{na'}\text{MX}_{x+n}$ , such that one of the two follows the predictions of dimensional reduction while the other does not. Note that this ratio will likely increase as more ternary compounds are characterized.
- (182) Hepworth, M. A.; Jack, K. H.; Peacock, R. D.; Westland, G. J. *Acta Crystallogr.* **1957**, *10*, 63–69.

CM0007858